Homogeneous Dirichlet wavelets on the interval diagonalizing the derivative operator, and related applications

Souleymane Kadri Harouna, Valérie Perrier

Homogeneous Dirichlet wavelets on the interval diagonalizing the derivative operator, and related applications

Souleymane Kadri Harouna[a,*], Valérie Perrier[b]

[a] *Laboratoire de Mathématiques, Image et Applications, Avenue Michel Crépeau, 17042 La Rochelle cedex 1 France.*
[b] *Univ. Grenoble Alpes, CNRS, Grenoble INP, LJK, 38000 Grenoble, France.*

Abstract

This paper presents a new construction of homogeneous Dirichlet wavelet basis on the unit interval, linked by a diagonal differentiation-integration relation to a standard biorthogonal wavelet basis. This new wavelet basis allows to compute the solution of the Poisson equation only by a wavelet coefficient renormalization - like in Fourier domain -, which yields a linear complexity $\mathcal{O}(N)$ for this problem. Another application concerns the construction of free-slip divergence-free wavelet bases of the hypercube, in general dimension, with an associated decomposition algorithm as simple as in the periodic case.

Keywords: Wavelets on the interval, Boundary condition, Poisson equation, Divergence-free wavelets

1. Introduction

Since the pioneering work of Lemarié-Rieusset [14], due to their important role in the construction of divergence-free or curl-free wavelets, biorthogonal multiresolution analyses linked by differentiation and integration have been widely studied [13, 19, 22, 23]. The main purpose was to construct two mul-

*Corresponding author
Email address: souleymane.kadri_harouna@univ-lr.fr (Souleymane Kadri Harouna)

tiresolution analyses of $L^2(0,1)$ provided by spaces V_j^1 and V_j^0 such that

$$\forall\ j,\quad \frac{d}{dx}V_j^1 = V_j^0. \tag{1}$$

Relation (1) should be interpreted as: $\forall f \in V_j^1$, $f' \in V_j^0$ and $\forall g \in V_j^0$, there exists $f \in V_j^1$ such that $f' = g$.

On the unit interval $[0,1]$, with non periodic boundary conditions, such a construction was firstly introduced by Jouini and Lemarié-Rieusset [13]. They started with V_j^1 as a *regular* multiresolution analysis of $L^2(0,1)$ reproducing polynomial at boundaries [1, 5, 11], with the scaling function φ^1 and wavelet ψ^1 generators on $\mathbb{R}$ that satisfy [14]:

$$(\varphi^1)' = \varphi^0 - \varphi^0(\cdot - 1) \quad \text{and} \quad (\psi^1)' = 4\psi^0. \tag{2}$$

Jouini and Lemarié-Rieusset [13] used the orthogonal construction of [5] for the space V_j^1. They show that, from relation (2) and properly setting the integer parameters in the construction of V_j^1, one can deduce the space V_j^0 that satisfies (1). In this case, the wavelet space W_j^0 is defined by differentiating the wavelet basis of W_j^1:

$$W_j^0 = span\{\psi_{j,k}^0 := 2^{-j}(\psi_{j,k}^1)'\}.$$

The corresponding biorthogonal spaces $(\tilde{V}_j^1, \tilde{V}_j^0)$ are respectively constructed again using integration by part. However, the construction of [13] remains theoretical, for instance it is not obvious to compute numerically the wavelet filters of $\psi_{j,k}^0$ and $\tilde{\psi}_{j,k}^0$:

$$\psi_{j,k}^0 = \sum_n H_{k,n}^0 \varphi_{j+1,n}^0 \quad \text{and} \quad \tilde{\psi}_{j,k}^0 = \sum_n \tilde{H}_{k,n}^0 \tilde{\varphi}_{j+1,n}^0. \tag{3}$$

where $V_j^0 = span\{\varphi_{j,k}^0; k\}$ and $\tilde{V}_j^0 = span\{\tilde{\varphi}_{j,k}^0; k\}$. This point has been raised by Kadri-Harouna and Perrier in [19], they extended the construction of [13] to any *regular* scaling function generator φ^1 and provided a numerical algorithm for the associated Fast Wavelet Transform.

One advantage of the construction [13, 19] is that the associated multiscale projectors commute with the derivative operator in $H^1(0,1)$. This fundamental property enables to construct divergence-free wavelet bases as it was done in [19]. Another interest of this property is to make possible the Ladysenskaya-Babuska-Brezzi (LBB) condition for a wavelet based method in the numerical discretization of a mixed problem such as the Stokes problem [3, 6]. The key ingredient is that, commutation with derivation allows to get easily the condition of Fortin's lemma [10], see [6].

Ensuring the commutation of multiscale projectors with differentiation imposes to the biorthogonal space $\tilde{V}_j^0$ to satisfy homogeneous Dirichlet boundary condition [13]. In this case, $\tilde{V}_j^0 \subset H_0^1(0,1)$ and constitutes a multiresolution analysis of this space (and not of $L^2(0,1)$). Nethertheless, relation (2) remains valid but only for internal scaling functions and wavelets (*i.e.* basis functions having their support included into $[0,1]$). The edge functions did not strictly satisfy this diagonal relation, but a linear combination of them: a change of basis is therefore introduced [20].

Recently, Stevenson [22] has proposed another construction which differs from the existing constructions by the choice of the boundary conditions for the dual spaces $\tilde{V}_j^0$ and $\tilde{V}_j^1$. Precisely, let us suppose that $\psi_{j,k}^1$ and $\tilde{\psi}_{j,k}^0$ are the wavelets constructed from scaling function generators satisfying (2). Then, integration by part shows that:

$$\psi_{j,k}^1(1)\tilde{\psi}_{j,k}^0(1) - \psi_{j,k}^1(0)\tilde{\psi}_{j,k}^0(0) = \langle \psi_{j,k}^0, \tilde{\psi}_{j,k}^0 \rangle - \langle \psi_{j,k}^1, \tilde{\psi}_{j,k}^1 \rangle. \tag{4}$$

If the two systems $(\psi_{j,k}^1, \tilde{\psi}_{j,k}^1)$ and $(\psi_{j,k}^0, \tilde{\psi}_{j,k}^0)$ are biorthogonal, the boundary terms of (4) should vanish. Instead of taking $\tilde{\psi}_{j,k}^0 \in H_0^1(0,1)$ like in [13], the construction of [22] sets $\psi_{j,k}^1(1) = 0$ and $\tilde{\psi}_{j,k}^0(0) = 0$. This choice of boundary condition is more flexible and leads to $\tilde{V}_j^0$ as a multiresolution analysis of $L^2(0,1)$: however the commutation of multiscale projectors with differentiation is lost. Alternatively, to get (4) one can take $(V_j^0, \tilde{V}_j^0)$ as a multiresolution of

$L_{2,0} = \{u \in L^2(0,1) \ : \ \int_0^1 u(t)dt = 0\}$ [21]. In this case, $V_j^1 = \int_0^x V_j^0 \subset H_0^1(0,1)$, thus only the spaces $\tilde{V}_j^1 = \frac{d}{dx}\tilde{V}_j^0$ can provide a multiresolution analysis of $L^2(0,1)$, see Proposition 3.1 of [21].

The focal point of this work is the construction of a wavelet basis satisfying homogeneous Dirichlet boundary conditions on the interval, associated to a biorthogonal multiresolution analyses of $H_0^1(0,1)$, and linked by a diagonal differentiation/integration relation to a standard wavelet bases of $H_0^1(0,1)$, as in[13, 19, 22]. As for the internal wavelets (2), emphasis is made on the construction of edge wavelets in order to get a diagonal differentiation relation:

$$\psi_{j,k}^1(x) = 2^j \int_0^x \psi_{j,k}^0(t)dt \quad \text{and} \quad (\psi_{j,k}^1)'(x) = 2^j \psi_{j,k}^0(x). \tag{5}$$

Contrarily to our previous construction [19], which started with the wavelets $\psi_{j,k}^1$ and $\tilde{\psi}_{j,k}^1$, in this work we begin with the knowledge of the wavelets $\psi_{j,k}^0$ and $\tilde{\psi}_{j,k}^0$: for this step, we will use a standard orthogonal or biorthogonal wavelet basis on the interval $[0,1]$ allowing polynomial reproduction even at boundaries, see e.g; [1, 5]. Since $\int_0^1 \psi_{j,k}^0(t)dt = 0$, relation (5) leads to $\psi_{j,k}^1 \in H_0^1(0,1)$ instead of $\psi_{j,k}^1 \in H^1(0,1)$ as in [13, 19, 22, 23]. Denoting by $\overline{W}_j^1$ this new wavelet spaces, one obtains the multiscale decompositions:

$$V_j^1 = V_{j_{min}}^1 \oplus \overline{W}_{j_{min}}^1 \oplus \cdots \oplus \overline{W}_{j-1}^1, \tag{6}$$

where incorporating homogeneous Dirichlet boundary condition in V_j^1 is reduced to the treatment of this boundary condition only at the coarse scale j_{min}:

$$V_j^1 \cap H_0^1(0,1) = \left(V_{j_{min}}^1 \cap H_0^1(0,1)\right) \oplus \overline{W}_{j_{min}}^1 \oplus \cdots \oplus \overline{W}_{j-1}^1, \tag{7}$$

Notice that, due to the property of polynomial reproduction at boundaries, the multiscale de composition (7) is stable in $H_0^1(0,1)$:

$$\|u\|_{H_0^1}^2 \sim \sum_{k \neq 0,1} | < u, \tilde{\varphi}_{j_{min},k}^1 > |^2 + \sum_{j \geq j_{min}} \sum_k 2^{2j} | < u, \tilde{\psi}_{j,k}^1 > |^2, \ \ \forall u \in H_0^1(0,1),$$

whereas (6) yields a non stable multiscale decomposition of $L^2(0,1)$.

Considering the particular case $\psi^0_{j,k} = \tilde{\psi}^0_{j,k}$, which corresponds to the orthogonal setting, leads to:

$$< (\psi^1_{j,k})', (\psi^1_{\ell,n})' >= 2^{j+\ell} < \psi^0_{j,k}, \psi^0_{\ell,n} >= 2^{j+\ell}\delta_{j,\ell}\delta_{k,n}. \tag{8}$$

Then, from (8) we infer that the 1D Poisson equation with homogeneous Dirichlet boundary can be solved with a linear numerical complexity in the multiresolution analysis provided by spaces V^1_j. Furthermore, this new construction still maintains the properties of Fortin's lemma [10] in the numerical discretization of Stokes problem and allows to get a fast divergence-free wavelet transform algorithm similar to this of the periodic case [9]. The main difficulty of such a construction is the numerical implementation of the decomposition (6), this point will be well documented in the present work.

In Section 2 we recall the construction of biorthogonal multiresolution analysis of $L^2(0,1)$ with polynomial reproduction and how to impose homogeneous boundary conditions in such context to obtain a basis of $H^1_0(0,1)$. Section 3 reminds the principle of the construction of BMRA linked by differentiation / integration and its main properties needed for a numerical implementation. The new construction of BMRA linked by differentiation / integration is detailed in Section 4, while the associated fast wavelet transform algorithms are provided in Section 5. Finally, Section 6 presents numerical examples showing the potentiality of these new bases.

2. Biorthogonal multiresolution analyses of $L^2(0,1)$ reproducing polynomial

The construction of biorthogonal multiresolution analyses $(V_j, \tilde{V}_j)$ of $L^2(0,1)$ with polynomial reproduction $(r, \tilde{r})$ is classical [4, 7, 11]: the principle is to start

with generators $(\varphi, \tilde{\varphi})$, that are biorthogonal scaling functions of a BMRA on $\mathbb{R}$. We suppose that φ is compactly supported on $[n_{min}, n_{max}]$ and reproduces polynomials up to degree $r-1$:

$$0 \leq \ell \leq r-1, \quad \frac{x^\ell}{\ell!} = \sum_{k=-\infty}^{+\infty} \tilde{p}_\ell(k)\ \varphi(x-k), \quad \forall\ x \in \mathbb{R}, \tag{9}$$

with $\tilde{p}_\ell(k) = \langle \frac{x^\ell}{\ell!}, \tilde{\varphi}(x-k) \rangle$. Similarly, $\tilde{\varphi}$ reproduces polynomials up to degree $\tilde{r}-1$ and we note $p_\ell(k) = \langle \frac{x^\ell}{\ell!}, \varphi(x-k) \rangle$. For j sufficiently large, the spaces V_j on $[0,1]$ have the structure:

$$V_j = V_j^\flat \oplus V_j^{int} \oplus V_j^\sharp, \tag{10}$$

where $V_j^{int} = span\{\varphi_{j,k}(x) = 2^{j/2}\varphi(2^j x - k)\ ;\ k = k_\flat,\ 2^j - k_\sharp\}$ is the space generated by *interior scaling functions* whose supports are included into $[\frac{\delta_\flat}{2^j}, 1 - \frac{\delta_\sharp}{2^j}] \subset [0,1]$ ($\delta_\flat,\ \delta_\sharp \in \mathbb{N}$ be two fixed parameters), and $k_\flat = \delta_\flat - n_{min}$ and $k_\sharp = \delta_\sharp + n_{max}$. Moreover

$$V_j^\flat = span\{\Phi_{j,\ell}^\flat(x) = 2^{j/2}\Phi_\ell^\flat(2^j x)\ ;\ \ell = 0, \cdots, r-1\},$$
$$V_j^\sharp = span\{\Phi_{j,\ell}^\sharp(1-x) = 2^{j/2}\Phi_\ell^\sharp(2^j(1-x))\ ;\ \ell = 0, \cdots, r-1\},$$

are the *edge spaces*, the *edge scaling functions* at the edge 0 being defined in order to preserve the polynomial reproduction (9) on the interval $[0,1]$:

$$0 \leq \ell \leq r-1, \qquad \Phi_\ell^\flat(x) = \sum_{k=1-n_{max}}^{k_\flat - 1} \tilde{p}_\ell(k)\ \varphi(x-k)\ \chi_{[0,+\infty[}. \tag{11}$$

At the edge 1, the edge scaling functions $\Phi_{j,\ell}^\sharp$ are constructed on $]-\infty, 1]$ by symmetry, using the transform $Tf(x) = f(1-x)$. In practice we have to choose $j \geq j_{min}$ where j_{min} is the smallest integer which verifies $j_{min} > \log_2[n_{max} - n_{min} + \delta_\sharp + \delta_\flat]$ to ensure that the supports of edge scaling functions at 0 do not intersect the supports of edge scaling functions at 1.

The polynomial reproduction in V_j is then satisfied since, for $0 \leq \ell \leq r-1$ and $x \in [0,1]$ we have:

$$\frac{2^{j/2}(2^j x)^\ell}{\ell!} = 2^{j/2}\Phi_\ell^\flat(2^j x) + \sum_{k=k_\flat}^{2^j - k_\sharp} \tilde{p}_\ell(k)\ \varphi_{j,k}(x) + 2^{j/2}\Phi_\ell^\sharp(2^j(1-x)). \tag{12}$$

Similarly, the biorthogonal spaces $\tilde{V}_j$ are defined with the same structure, allowing the polynomial reproduction up to degree $\tilde{r}-1$:

$$\tilde{V}_j = span\{\tilde{\Phi}^{\flat}_{j,\ell}\}_{\ell=0,\tilde{r}-1} \oplus \tilde{V}_j^{int} \oplus span\{\tilde{\Phi}^{\sharp}_{j,\ell}\}_{\ell=0,\tilde{r}-1}, \tag{13}$$

where $\tilde{V}_j^{int} = span\{\tilde{\varphi}_{j,k}\ ;\ k=\tilde{k}_{\flat},\ 2^j-\tilde{k}_{\sharp}\}$ is the space generated by interior scaling functions $\tilde{\varphi}_{j,k}(x) = 2^{j/2}\tilde{\varphi}^1(2^j x-k)$, whose supports are included into $[\frac{\tilde{\delta}_{\flat}}{2^j}, 1-\frac{\tilde{\delta}_{\sharp}}{2^j}]$ ($\tilde{\delta}_{\flat},\ \tilde{\delta}_{\sharp} \in \mathbb{N}$ be two parameters). The edge scaling functions at 0 are defined by:

$$0 \le \ell \le \tilde{r}-1, \qquad \tilde{\Phi}^{\flat}_{\ell}(x) = \sum_{k=1-\tilde{n}_{max}}^{\tilde{k}_{\flat}-1} p_{\ell}(k)\ \tilde{\varphi}(x-k)\ \chi_{[0,+\infty[}.$$

The equality between dimensions of V_j and $\tilde{V}_j$ is obtained by adjusting the parameters $\tilde{\delta}_{\flat} = \tilde{k}_{\flat} - \tilde{n}_{max}$ and $\tilde{\delta}_{\sharp} = \tilde{k}_{\sharp} + \tilde{n}_{min}$ (with $[\tilde{n}_{min}, \tilde{n}_{max}] = supp\ \tilde{\varphi}$) such that: $\Delta_j = \dim(V_j) = \dim(\tilde{V}_j) = 2^j - (\delta_{\flat}+\delta_{\sharp}) - (n_{max}-n_{min}) + 2r + 1$. Remark that $(\delta_{\flat},\ \delta_{\sharp})$ remain "free" parameters of the construction (often chosen equal to 0 or 1). The last step of the construction lies in the biorthogonalization process of the basis functions, since edge scaling functions of V_j and $\tilde{V}_j$ are no more biorthogonal [1, 7, 11, 16]. Finally, the spaces $(V_j, \tilde{V}_j)$ form a biorthogonal MRA of $L^2(0,1)$.

Boundary conditions. A multiresolution analyses of

$$H_0^m(0,1) = \{f \in H^m(0,1)\ :\ f^{(p)}(0) = f^{(p)}(1) = 0,\quad 0 \le p \le m-1\}$$

can be defined from V_j by taking $V_j^{m,0} = V_j \cap H_0^m(0,1)$. For instance, if $m=1$, as described in [15, 16], it suffices to remove the edge scaling functions $\Phi_0^{\flat}$ at edge 0 and $\Phi_0^{\sharp}$ at edge 1 which leads to:

$$V_j^{1,0} = span\{\Phi^{\flat}_{j,\ell}\ ;\ \ell=1,r-1\} \oplus V_j^{int} \oplus span\{\Phi^{\sharp}_{j,\ell}\ ;\ \ell=1,r-1\}.$$

In such case, we also remove the edge functions $\tilde{\Phi}_0^{\flat}$ and $\tilde{\Phi}_0^{\sharp}$ from $\tilde{V}_j$ prior to biorthogonalization, to adjust the dimension of the biorthogonal space. Then, the spaces $(V_j^{1,0}, \tilde{V}_j^{1,0})$ constitute a biorthogonal multiresolution analyses of $H_0^1(0,1)$.

3. Existing construction of $(V_j^0, \tilde{V}_j^0)$ linked by differentiation / integration with $(V_j^1, \tilde{V}_j^1)$

In this section, we recall briefly the earlier construction of the multiresolution analysis linked differentiation / integration. Then, we will mention their limitations in some applications that we intend to take up with our new construction below.

All the constructions of biorthogonal multiresolution analyses of $L^2(0,1)$ linked by differentiation / integration are based on the following proposition [14]:

Proposition 1. *Let $(V_j^1(\mathbb{R}), \tilde{V}_j^1(\mathbb{R}))$ be a biorthogonal MRA of $L^2(\mathbb{R})$, with associated scaling functions $\varphi^1, \tilde{\varphi}^1$ and wavelets $\psi^1, \tilde{\psi}^1$. Assume that $V_j^1(\mathbb{R})$ is regular, $\varphi^1 \in \mathcal{C}^{1+\epsilon}$, $\epsilon > 0$, and compactly supported. Then there exists a biorthogonal MRA $(V_j^0(\mathbb{R}), \tilde{V}_j^0(\mathbb{R}))$, with associated scaling functions $\varphi^0, \tilde{\varphi}^0$ and wavelets $\psi^0, \tilde{\psi}^0$, such that:*
$(\varphi^1)'(x) = \varphi^0(x) \; - \; \varphi^0(x-1)$ *and* $(\psi^1)' \; = \; 4 \; \psi^0$.
The biorthogonal functions verify: $\int_x^{x+1} \tilde{\varphi}^1(t) \; dt = \tilde{\varphi}^0(x)$ *and* $(\tilde{\psi}^0)' \; = \; -4 \; \tilde{\psi}^1$.

Proposition 1 provides biorthogonal multiresolution analysis of $L^2(\mathbb{R})$ linked by differentiation/ integration [14]. For the space $L^2(0,1)$, again based on Proposition 1, the first construction was done by Jouini and Lemarié-Rieusset [13]: they prove the existence of two biorthogonal multiresolution analyses of $L^2(0,1)$, denoted (V_j^1) and (V_j^0) linked by differentiation such that:

$$\frac{d}{dx} V_j^1 \quad = \quad V_j^0. \tag{14}$$

The construction of [13] allows to study divergence-free vector functions on hypercube $[0,1]^d$, thus to get commutation of multiscale projector with the derivation operator, the biorthogonal spaces $\tilde{V}_j^0$ should satisfy:

$$\tilde{V}_j^0 \quad = \quad H_0^1(0,1) \cap \int_0^x \tilde{V}_j^1 = \left\{ f \; : \; f' \in \tilde{V}_j^1 \text{ and } \; f(0) = f(1) = 0 \right\}. \tag{15}$$

Then, as mentioned before, $\tilde{V}_j^0$ can not be a multiresolution analysis of $L^2(\mathbb{R})$

since $\tilde{V}_j^0 \subset H_0^1(0,1)$. Furthermore, if $(\mathcal{P}_j^1, \tilde{\mathcal{P}}_j^1)$ are the biorthogonal projectors of $(V_j^1, \tilde{V}_j^1)$ and $(\mathcal{P}_j^0, \tilde{\mathcal{P}}_j^0)$ those of $(V_j^0, \tilde{V}_j^0)$ respectively, we have [13]:

Proposition 2.

(i) $\forall\ f \in H^1(0,1), \quad \frac{d}{dx} \circ \mathcal{P}_j^1 f = \mathcal{P}_j^0 \circ \frac{d}{dx} f,$

(ii) $\forall\ f \in H_0^1(0,1), \quad \frac{d}{dx} \circ \tilde{\mathcal{P}}_j^0 f = \tilde{\mathcal{P}}_j^1 \circ \frac{d}{dx} f.$

Despite of satisfying Proposition 2, the construction of Jouini and Lemarié-Rieusset [13] remains in a theoretical setting and inspired by the use of Daubechies compactly supported orthogonal generators [8]. A construction that uses classical biorthogonal multiresolution analyses on the interval [4, 7, 11], with polynomial reproduction at boundaries, was done and implemented by Kadri-Harouna and Perrier [19]. In such a construction, the choice of integer parameters $(\delta_\flat, \delta_\sharp)$ and $(\tilde{\delta}_\flat, \tilde{\delta}_\sharp)$ is very important: they must be identical for the two multiresolution analyses to satisfy (14,15) and to provide the commutation of multiscale projectors with the differentiation operator.

3.1. Wavelet spaces

For $j \geq j_{min}$, the biorthogonal wavelet spaces associated to V_j^1 are defined by $W_j^1 = V_{j+1}^1 \cap (\tilde{V}_j^1)^\perp$. As for the scaling function spaces, these spaces have the following structure:

$$W_j^1 = W_j^{1,\flat} \oplus W_j^{1,int} \oplus W_j^{1,\sharp},$$

where $W_j^{1,\flat}$ is spanned by the edge wavelets at 0, $W_j^{1,int}$ is spanned by the interior wavelets and $W_j^{1,\sharp}$ is spanned by the edge wavelets at 1, see [1, 4, 7, 11, 16] and references therein. The biorthogonal spaces $\tilde{W}_j^1 = \tilde{V}_{j+1}^1 \cap (V_j^1)^\perp$ are constructed in the same way, finally the wavelet bases of the two spaces must to be biorthogonalized identically as the scaling functions. The resulting wavelet bases are denoted by $\{\psi_{j,k}^1\}_{k=1,2^j}$ and $\{\tilde{\psi}_{j,k}^1\}_{k=1,2^j}$ without distinction.

The biorthogonal wavelets of W_j^0 and $\tilde{W}_j^0$, linked to $\psi_{j,k}^1$ and $\tilde{\psi}_{j,k}^1$ by differentiation/integration are defined by the following proposition, established in the general framework by [13]:

Proposition 3. *Let $(V_j^1, \tilde{V}_j^1)$ and $(V_j^0, \tilde{V}_j^0)$ BMRAs satisfying (14,15). The wavelet spaces $W_j^0 = V_{j+1}^0 \cap (\tilde{V}_j^0)^\perp$ and $\tilde{W}_j^0 = \tilde{V}_{j+1}^0 \cap (V_j^0)^\perp$ are linked to the biorthogonal wavelet spaces associated to $(V_j^1, \tilde{V}_j^1)$ by:*

$$W_j^0 = \frac{d}{dx} W_j^1 \quad \textit{and} \quad \tilde{W}_j^0 = \int_0^x \tilde{W}_j^1. \tag{16}$$

Moreover, let $\{\psi_{j,k}^1\}_{k=1,2^j}$ and $\{\tilde{\psi}_{j,k}^1\}_{k=1,2^j}$ be two biorthogonal wavelet bases of W_j^1 and $\tilde{W}_j^1$. Biorthogonal wavelet bases of W_j^0 and $\tilde{W}_j^0$ are directly defined by:

$$\psi_{j,k}^0 = 2^{-j} (\psi_{j,k}^1)' \quad \textit{and} \quad \tilde{\psi}_{j,k}^0 = -2^j \int_0^x \tilde{\psi}_{j,k}^1. \tag{17}$$

This new edge wavelets preserve fast algorithms since they satisfy two-scale equations [19]:

Proposition 4. *Let $\{\psi_{j,k}^1\}_{k=1,2^j}$ and $\{\tilde{\psi}_{j,k}^1\}_{k=1,2^j}$ be two biorthogonal wavelet bases of W_j^1 and $\tilde{W}_j^1$ associated respectively to filters G_j^1 and $\tilde{G}_j^1$:*

$$\psi_{j,k}^1 = \sum_n (G_j^1)_{k,n} \; \varphi_{j+1,n}^1 \quad \textit{and} \quad \tilde{\psi}_{j,k}^1 = \sum_n (\tilde{G}_j^1)_{k,n} \; \tilde{\varphi}_{j+1,n}^1.$$

Then there exist sparse matrices G_j^0 and $\tilde{G}_j^0$ defined by:

$$G_j^0 = 2^{-j} G_j^1 L_{j+1}^1 \quad \textit{and} \quad \tilde{G}_j^0 = -2^j \tilde{G}_j^1 L_{j+1}^{0T}, \tag{18}$$

such that the wavelets $\psi_{j,k}^0$ and $\tilde{\psi}_{j,k}^0$ satisfy:

$$\psi_{j,k}^0 = \sum_n (G_j^0)_{k,n} \varphi_{j+1,n}^0 \quad \textit{and} \quad \tilde{\psi}_{j,k}^0 = \sum_n (\tilde{G}_j^0)_{k,n} \tilde{\varphi}_{j+1,n}^0.$$

The matrices L_j^1 and L_j^0 correspond to the change of basis between $(\frac{d}{dx} V_j^1, V_j^0)$ and $(\int_0^x V_j^0, V_j^1)$, respectively:

$$\frac{d}{dx} \varphi_{j,k}^1 = \sum_{n=1}^{\Delta_j - 1} (L_j^1)_{k,n} \; \varphi_{j,n}^0 \quad \textit{and} \quad -\int_0^x \varphi_{j,k}^0 = \sum_{m=1}^{\Delta_j} (L_j^0)_{k,m} \; \varphi_{j,m}^1. \tag{19}$$

Interior wavelets $\psi^0_{j,k}(x) = 2^{j/2}\psi^0(2^j x - k)$ in Proposition 3 correspond to classical wavelets, ψ^0 being a wavelet on $\mathbb{R}$ associated to the scaling function φ^0 as in Proposition 1.

In the previous works [19, 22], to construct divergence-free wavelet satisfying *free slip* boundary condition, one needs to differentiate wavelets of $V^1_{j+1} \cap H^1_0(0,1)$ that satisfy homogeneous Dirichlet boundary condition, which derivatives differ from the wavelets defined in (17). In this case, the numerical computation of the Helmholtz-Hodge decomposition or the numerical simulation of the incompressible Navier-Stokes equations should required the use of four different kind of edge wavelet filters. Precisely, in two space dimension using the multiresolution analysis $(V^1_j \otimes V^0_j) \times (V^0_j \otimes V^1_j)$, one should use the wavelet filters of $(\psi^1_{j,k}; \psi^0_{j,k} = 2^{-j}(\psi^1_{j,k})')$ for the usual decomposition and the wavelet filters of $(\psi^{1,0}_{j,k} \in V^1_{j+1} \cap H^1_0(0,1); 2^{-j}(\psi^{1,0}_{j,k})' \neq \psi^0_{j,k})$, due to the *free slip* boundary condition, see [18, 20] for details.

The new construction detailed in the next section will lead to edge wavelets that satisfy relation (17) even if with homogeneous Dirichlet boundary condition.

4. New construction of $(V^1_j, \tilde{V}^1_j)$ linked to $(V^0_j, \tilde{V}^0_j)$ by differentiation / integration to handle boundary conditions in V^1_j.

In this section we present our new construction of biorthogonal multiresolution analyses linked by differentiation and integration. The construction of the primal spaces (V^1_j, V^0_j) remains the same as in the classical construction [13, 19]. However, the construction of the *biorthogonal* spaces $(\tilde{V}^1_j, \tilde{V}^0_j)$ will be different. Indeed, to handle Dirichlet boundary conditions in V^1_j, we will construct new wavelet bases $(\psi^1_{j,k})$ which will constitue a Riesz basis for the homogeneous space $H^1_0(0,1)$. This is an issue of major benefit in the construction of divergence-free

wavelet satisfying physical boundary condition [19].

The construction starts with $(V_j^0, \tilde{V}_j^0)$ as a standard biorthogonal multiresolution analyses of $L^2(0,1)$ [1, 4, 5] (which can be orthogonal), where the scaling function generators $(\varphi^0, \tilde{\varphi}^0)$ satisfy Proposition 1, with at least two vanishing moments for the wavelet ψ^0: $\tilde{r}^0 \geq 2$. We denote by $(\delta_\flat, \delta_\sharp)$ and $(\tilde{\delta}_\flat, \tilde{\delta}_\sharp)$ the integer parameters used in the construction of $(V_j^0, \tilde{V}_j^0)$. Following [13, 19], the classical multiresolution spaces V_j^1 is constructed from the scaling function generator φ^1 with the same integer parameters $(\delta_\flat, \delta_\sharp)$ and satisfy:

$$\frac{d}{dx} V_j^1 = V_j^0 \quad \text{and} \quad \Delta_j^1 - 1 = \Delta_j^0.$$

In this case, for the biorthogonal space $\tilde{V}_j^0$, since $\Delta_j^0 = dim(\tilde{V}_j^0)$, we see that:

$$\Delta_j^1 - 2 = dim(\frac{d}{dx} \tilde{V}_j^0).$$

The construction of $\tilde{V}_j^1$ follows similar approach with the generator $\tilde{\varphi}^1$. To get equality between dimensions of spaces V_j^1 and $\tilde{V}_j^1$ one needs:

$$\Delta_j^1 = \tilde{\Delta}_j^1,$$

which imposes to the integer parameters to be used for the construction of $\tilde{V}_j^1$ to be fixed to $(\tilde{\delta}_\flat - 1, \tilde{\delta}_\sharp - 1)$. It follows therefore that:

$$\frac{d}{dx} \tilde{V}_j^0 \not\subset \tilde{V}_j^1.$$

This is a major difference compared to the existing construction.

4.1. A new wavelet space for V_j^1

The construction of the wavelet basis associated to V_j^1 is the major contribution of the present work. In the classical construction, on defines the wavelet space as:

$$V_{j+1}^1 = V_j^1 \oplus W_j^1, \quad \text{where} \quad W_j^1 = V_{j+1}^1 \cap (\tilde{V}_j^1)^\perp.$$

Then, the space W_j^1 does not necessarily satisfy homogeneous Dirichlet boundary condition. To compensate for that, in this work the wavelet space is defined

as:

$$\overline{W}_j^1 = \int_0^x W_j^0,$$

where W_j^0 is the wavelet space associated to V_j^0 [1, 4, 7, 11, 16]:

$$W_j^0 = V_{j+1}^0 \cap (\tilde{V}_j^0)^\perp.$$

Remark 1.

From the zero mean value property of the wavelet $\psi_{j,k}^0$, by construction the space $\overline{W}_j^1$ satisfies:

$$\overline{W}_j^1 \subset H_0^1(0,1).$$

In the previous section, the wavelet space W_j^0 was defined as $W_j^0 = \frac{d}{dx} W_j^1$ and this choice of W_j^0 led in general to:

$$W_j^1 \neq \int_0^x W_j^0.$$

183 For all $j \geq j_{min}$, the spaces $\overline{W}_j^1$ verify the following proposition.

Proposition 5.

Let W_j^0 be the wavelet space associated to V_j^0, where $V_j^0 = \frac{d}{dx} V_j^1$. Then the space V_{j+1}^1 can be decomposed as follows:

$$V_{j+1}^1 = V_j^1 \oplus \overline{W}_j^1, \quad \textit{with} \quad \overline{W}_j^1 = \int_0^x W_j^0 \ , \tag{20}$$

and

$$V_{j+1}^1 = V_{j_{min}}^1 \oplus \overline{W}_{j_{min}}^1 \oplus \cdots \oplus \overline{W}_j^1. \tag{21}$$

Proof. As $\frac{d}{dx} V_j^1 = V_j^0$, we get:

$$\overline{W}_j^1 = \int_0^x W_j^0 \subset \int_0^x \frac{d}{dt} V_{j+1}^1 \subset V_{j+1}^1 \quad \text{and} \quad \int_0^x W_j^0 \subset H_0^1(0,1).$$

Moreover, let u_j be a function of $V_j^1 \cap \overline{W}_j^1$:

$$u_j = \sum_k c_k \varphi_{j,k}^1 = \sum_n d_n \int_0^x \psi_{j,n}^0,$$

we deduce that:

$$\frac{d}{dx} u_j \in V_j^0 \cap W_j^0 \ \Rightarrow \ \frac{d}{dx} u_j = 0 \ \Rightarrow \ u_j = C \in \mathbb{R}.$$

Since

$$\langle 1, \int_0^x \psi_{j,n}^0 \rangle = -\langle x, \psi_{j,n}^0 \rangle = 0,$$

we get $u_j = 0$, which implies $V_j^1 \cap \overline{W}_j^0 = \{0\}$. Let $f_{j+1} \in V_{j+1}^1$, then:

$$\frac{d}{dx} f_{j+1} \in V_{j+1}^0 = V_j^0 \oplus W_j^0.$$

Since $f_{j+1}(0) \in V_j^1$ (the constants are in V_j^1), integration gives:

$$f_{j+1}(x) = f_{j+1}(0) + \int_0^x \mathcal{P}_j^0(\frac{d}{dx} f_{j+1}) + \int_0^x \mathcal{Q}_j^0(\frac{d}{dx} f_{j+1}) \in V_j^1 + \overline{W}_j^1,$$

and this ends the proof. □

4.2. A new multiscale decomposition of $H_0^1(0,1)$, and relation with the derivative operator

We recall that from the results of Section 2, incorporating homogeneous boundary conditions in V_j^1 consists on removing the two scaling functions that do not satisfy the desired boundary conditions. In addition to that, one interest of this new wavelet space construction is that the treatment of homogeneous Dirichlet boundary conditions in V_j^1 is done only at the coarse scale j_{min}. Indeed, by construction the space $\overline{W}_j^1 = \int_0^x W_j^0 \subset H_0^1(0,1)$ and relation (21) allow to get the following decomposition:

$$V_{j+1}^{1,0} = V_{j+1}^1 \cap H_0^1(0,1) = \left(V_{j_{min}}^1 \cap H_0^1(0,1)\right) \oplus \overline{W}_{j_{min}}^1 \oplus \cdots \oplus \overline{W}_j^1. \qquad (22)$$

Moreover, as a matter of fact, the wavelet space $\overline{W}_j^1$ is the classical wavelet space of $H_0^1(0,1)$ associated to the multiresolution analysis constituted by $V_j^{1,0}$ (but the wavelet basis is different), as proved in the following proposition.

Proposition 6.

Let $(V_j^1, \tilde{V}_j^1)$ and $(V_j^0, \tilde{V}_j^0)$ be two BMRAs of $L^2(0,1)$ linked by differentiation and integration constructed using the parameters $(\delta_\flat, \delta_\sharp)$ and $(\tilde{\delta}_\flat, \tilde{\delta}_\sharp)$. Defining the biorthogonal spaces $(V_j^{1,0}, \tilde{V}_j^{1,0})$ by:

$$V_j^{1,0} = V_j^1 \cap H_0^1(0,1) \quad \textit{and} \quad \frac{d}{dx} \tilde{V}_j^0 = \tilde{V}_j^{1,0}, \qquad (23)$$

then we have:

- *(i) The spaces $V_j^{1,0}$ provide a multiresolution analysis of $H_0^1(0,1)$.*
- *(ii) The space $\overline{W}_j^1 = \int_0^x W_j^0$ is the classical wavelet space associated to $V_j^{1,0}$:*

$$V_{j+1}^{1,0} = V_{j+1}^1 \cap H_0^1(0,1) = V_j^{1,0} \oplus \int_0^x W_j^0 \quad \textit{and} \quad \int_0^x W_j^0 = V_{j+1}^{1,0} \cap (\tilde{V}_j^{1,0})^\perp. \tag{24}$$

Proof.

The first point (i) is evident. Since V_j^1 is a multiresolution analysis of $L^2(0,1)$ and $V_{j_{min}}^{1,0} = V_{j_{min}}^1 \cap H_0^1(0,1)$, we have:

$$\overline{\cup_{j \geq j_{min}} V_j^{1,0}} = H_0^1(0,1). \tag{25}$$

For the second point (ii), from the vanishing moment condition of the wavelet basis of W_j^0 we get:

$$\int_0^1 W_j^0 = 0 \quad \Rightarrow \quad \int_0^x W_j^0 \subset H_0^1(0,1).$$

The differentiation relation gives:

$$\frac{d}{dx} V_{j+1}^1 = V_{j+1}^0 \quad \Rightarrow \quad \int_0^x V_{j+1}^0 \subset V_{j+1}^1,$$

thus

$$\int_0^x W_j^0 \subset V_{j+1}^1 \cap H_0^1(0,1) = V_{j+1}^{1,0}.$$

Moreover, the differentiation relation:

$$\frac{d}{dx} \tilde{V}_j^0 = \tilde{V}_j^{1,0}$$

states that for any $\tilde{f}_j^{1,0} \in \tilde{V}_j^{1,0}$, there exists $\tilde{f}_j^0 \in \tilde{V}_j^0$ such that $(\tilde{f}_j^0)' = \tilde{f}_j^{1,0}$, then:

$$\langle \int_0^x \psi_{j,k}^0, \tilde{f}_j^{1,0} \rangle = \langle \int_0^x \psi_{j,k}^0, \frac{d}{dx} \tilde{f}_j^0 \rangle = -\langle \psi_{j,k}^0, \tilde{f}_j^0 \rangle = 0 \quad \Rightarrow \quad \int_0^x W_j^0 \subset (\tilde{V}_j^{1,0})^\perp.$$

Then we deduce that

$$\int_0^x W_j^0 \subset V_{j+1}^{1,0} \cap (\tilde{V}_j^{1,0})^\perp$$

and since the two spaces have the same dimension, we get:

$$\int_0^x W_j^0 = V_{j+1}^{1,0} \cap (\tilde{V}_j^{1,0})^{\perp}.$$

□

We remind that the integer parameters used in the construction of $\tilde{V}_j^1$ and $\tilde{V}_j^0$ are not the same. Then one can not expect to get commutation between multiscale projectors and derivation as in Proposition 2, but for the oblique multiscale projectors of $(V_j^{1,0}, V_j^0)$ and $(\tilde{V}_j^0, \tilde{V}_j^{1,0})$ we can prove the following proposition:

Proposition 7.
Let $(\mathcal{P}_j^{1,0}, \mathcal{P}_j^0)$ be the biorthogonal projectors associated with $(V_j^{1,0}, V_j^0)$ and $(\widetilde{\mathcal{P}}_j^0, \widetilde{\mathcal{P}}_j^{1,0})$ the biorthogonal projectors associated with $(\tilde{V}_j^0, \tilde{V}_j^{1,0})$. Then, we have:

(i) $\forall\ f \in H_0^1(0,1), \quad \frac{d}{dx} \circ \mathcal{P}_j^{1,0} f = \mathcal{P}_j^0 \circ \frac{d}{dx} f.$

(ii) $\forall\ f \in H^1(0,1), \quad \frac{d}{dx} \circ \tilde{\mathcal{P}}_j^0 f = \tilde{\mathcal{P}}_j^{1,0} \circ \frac{d}{dx} f.$

Proof.

From proposition 6, there exist two matrices denoted $L_j^{1,0}$ and $\widetilde{L}_j^{1,0}$ of size $(\Delta_j^1 - 2) \times (\Delta_j^1 - 1)$, such that:

$$\varphi_{j,k}^{1,0} = \sum_{n=1}^{\Delta_j^1 - 1} (L_j^{1,0})_{k,n} \int_0^x \varphi_{j,n}^0 \qquad \text{and} \qquad \int_0^x \tilde{\varphi}_{j,k}^{1,0} = \sum_{n=1}^{\Delta_j^1 - 1} (\widetilde{L}_j^{1,0})_{k,n}\ \tilde{\varphi}_{j,n}^0. \quad (26)$$

Then, the biorthogonality of the basis functions $\varphi_{j,k}^{1,0}$ and $\tilde{\varphi}_{j,k}^{1,0}$, with an integration by part give:

$$\begin{aligned} \delta_{k,m} &= \langle \varphi_{j,k}^{1,0}, \tilde{\varphi}_{j,m}^{1,0} \rangle = \sum_{\ell} (\widetilde{L}_j^{1,0})_{m,\ell} \langle \varphi_{j,k}^{1,0}, \frac{d}{dx} \tilde{\varphi}_{j,\ell}^0 \rangle = \sum_{\ell} (\widetilde{L}_j^{1,0})_{m,\ell} \langle -\frac{d}{dx} \varphi_{j,k}^{1,0}, \tilde{\varphi}_{j,\ell}^0 \rangle \\ &= -\sum_n \sum_{\ell} (L_j^{1,0})_{k,n} (\widetilde{L}_j^{1,0})_{m,\ell} \langle \varphi_{j,n}^0, \tilde{\varphi}_{j,\ell}^0 \rangle = -\sum_n (L_j^{1,0})_{k,n} (\widetilde{L}_j^{1,0})_{m,n}, \end{aligned}$$

which means that:

$$I_{\Delta_j - 2} = -L_j^{1,0}\ {}^t\widetilde{L}_j^{1,0}.$$

Thus, the proof of the point (i) becomes a change of basis. Indeed, for $f \in H_0^1(0,1)$, we have:

$$\begin{aligned}
\frac{d}{dx}\mathcal{P}_j^{1,0}(f) &= \sum_k \langle f, \tilde{\varphi}_{j,k}^{1,0}\rangle \ \frac{d}{dx}\varphi_{j,k}^{1,0} = \sum_k \sum_n (L_j^{1,0})_{k,n} \langle f, \tilde{\varphi}_{j,k}^{1,0}\rangle \ \varphi_{j,n}^0 \\
&= \sum_n \langle f, \sum_k (L_j^{1,0})_{k,n} \tilde{\varphi}_{j,k}^{1,0}\rangle \ \varphi_{j,n}^0 = \sum_n \langle f, \sum_k \sum_m (L_j^{1,0})_{k,n} (\widetilde{L}_j^{1,0})_{k,m} \frac{d}{dx}\tilde{\varphi}_{j,m}^0\rangle \ \varphi_{j,n}^0 \\
&= \sum_n \langle f, -\frac{d}{dx}\tilde{\varphi}_{j,n}^0\rangle \ \varphi_{j,n}^0 = \sum_n \langle \frac{d}{dx} f, \tilde{\varphi}_{j,n}^0\rangle \ \varphi_{j,n}^0 = \mathcal{P}_j^0(\frac{d}{dx} f).
\end{aligned}$$

For the second point (ii), let us consider the matrix $\widetilde{L}_j^0$ defined by:

$$\frac{d}{dx}\tilde{\varphi}_{j,k}^0 = \sum_{n=1}^{\Delta_j^0 - 1} (\widetilde{L}_j^0)_{k,n} \ \tilde{\varphi}_{j,n}^{1,0}.$$

Again, the duality of the basis and integration by part give:

$$\langle \frac{d}{dx}\varphi_{j,k}^{1,0}, \tilde{\varphi}_{j,m}^0\rangle = (L_j^{1,0})_{k,m} = \langle \varphi_{j,k}^{1,0}, -\frac{d}{dx}\tilde{\varphi}_{j,m}^0\rangle = -(\tilde{L}_j^0)_{m,k},$$

then

$$\begin{aligned}
\frac{d}{dx}\tilde{\mathcal{P}}_j^0(f) &= \sum_k \langle f, \varphi_{j,k}^0\rangle \ \frac{d}{dx}\tilde{\varphi}_{j,k}^0 = \sum_k \sum_n (\tilde{L}_j^0)_{k,n} \langle f, \varphi_{j,k}^0\rangle \ \tilde{\varphi}_{j,n}^{1,0} \\
&= \sum_n \langle f, \sum_k (\tilde{L}_j^0)_{k,n} \varphi_{j,k}^0\rangle \ \tilde{\varphi}_{j,n}^{1,0} = \sum_n \langle f, -\sum_k (\tilde{L}_j^{1,0})_{n,k} \varphi_{j,k}^0\rangle \ \tilde{\varphi}_{j,n}^{1,0} \\
&= \sum_n \langle f, -\frac{d}{dx}\varphi_{j,n}^{1,0}\rangle \ \tilde{\varphi}_{j,n}^{1,0} = \sum_n \langle \frac{d}{dx} f, \varphi_{j,n}^{1,0}\rangle \ \tilde{\varphi}_{j,n}^{1,0} = \tilde{\mathcal{P}}_j^{1,0}(\frac{d}{dx} f).
\end{aligned}$$

□

4.3. Fast decomposition algorithm

In this section we provide the decomposition of a given function $f \in H_0^1(0,1)$ in the MRA $(V_j^{1,0})$ using (25, 22). As usual in Fast Wavelet Transforms, the complete decomposition uses a binary tree whose elementary step is given by the decomposition:

$$V_{j+1}^{1,0} = V_j^{1,0} \oplus \overline{W}_j^1 \tag{27}$$

Remembering that the space $V_j^{1,0}$ is obtained from V_j^1 only removing one boundary scaling function at each boundary 0 and 1:

$$V_j^{1,0} = span\{\varphi_j^{1,0}; j = 2, \cdots, \Delta_j^1 - 1\}$$

and that (22) holds, we first study the elementary step:

$$V_{j+1}^1 = V_j^1 \oplus \overline{W}_j^1.$$

Therefore we will study the computation of the projection of $f_{j+1} \in V_{j+1}^1$ onto V_j^1 and $\overline{W}_j^1$ respectively. Precisely, starting with:

$$f_{j+1} = \sum_{k=1}^{\Delta_{j+1}^1} c_{j+1,k}\varphi_{j+1,k}^1,$$

we want to compute the coefficients $c_{j,k}$ and $d_{j,k}$ from $c_{j+1,k}$ such that:

$$f_{j+1} = \sum_{k=1}^{\Delta_j^1} c_{j,k}\varphi_{j,k}^1 + \sum_{m=1}^{2^j} d_{j,m} \int_0^x \psi_{j,m}^0.$$

Firstly, we notice that f_{j+1} can be split as

$$f_{j+1} = \sum_{k=1}^{\Delta_{j+1}^1} c_{j+1,k}\varphi_{j+1,k}^1 = f_{j+1}^0 + f_{j+1}^{1,0} + f_{j+1}^1,$$

with

$$f_{j+1}^0 = c_{j+1,1}\varphi_{j+1,1}^1 \quad \Rightarrow \quad f_{j+1}^0(0) \neq 0 \ \text{ and } \ f_{j+1}^0(1) = 0,$$

$$f_{j+1}^1 = c_{j+1,\Delta_{j+1}^1}\varphi_{j+1,\Delta_{j+1}^1}^1 \quad \Rightarrow \quad f_{j+1}^1(0) = 0 \ \text{ and } \ f_{j+1}^1(1) \neq 0,$$

and

$$f_{j+1}^{1,0} = \sum_{k=2}^{\Delta_{j+1}^1 - 1} c_{j+1,k}\varphi_{j+1,k}^1 \in V_{j+1}^{1,0} \subset H_0^1(0,1).$$

Thus, the two scale decomposition of $f_{j+1}^{1,0}$ is a classical decomposition in the multiresolution analysis of $H_0^1(0,1)$ provided by the scaling function filter of $V_j^{1,0}$ and wavelet filter of $\overline{W}_j^1$. To compute the projection of f_{j+1}^0, one way to proceed is to use the two scale relations satisfied by $\varphi_{j+1,1}^1$:

$$\varphi_{j+1,1}^1 = \sum_{n=1}^{\tilde{\Delta}_j^1} \tilde{H}_{n,1}^1\varphi_{j,n}^1 + \sum_{m=1}^{2^j} \tilde{G}_{m,1}^1\psi_{j,m}^1 = \sum_{n=1}^{\tilde{\Delta}_j^1} \tilde{\overline{H}}_{n,1}^1\varphi_{j,n}^1 + \sum_{m=1}^{2^j} \tilde{\overline{G}}_{m,1}^1 \int_0^x \psi_{j,m}^0,$$

where the first decomposition corresponds to $V_{j+1}^1 = V_j^1 \oplus W_j^1$, with W_j^1 a chosen classical wavelet space associated to V_j^1 [4, 7, 11, 16] and the second one corresponds to $V_{j+1}^1 = V_j^1 \oplus \overline{W}_j^1$.

Then, to get the new filters $\tilde{\overline{H}}_{n,1}^1$ and $\tilde{\overline{G}}_{n,1}^1$, according to the biorthogonalization procedure that we adopted, where only the dual basis are modified, we have:

$$\tilde{G}_{k,1}^1 = \sum_{m=1}^{2^j} \tilde{\overline{G}}_{m,1}^1 \langle \int_0^x \psi_{j,m}^0, \tilde{\psi}_{j,k}^1 \rangle, \tag{28}$$

and

$$\tilde{H}_{k,1}^1 = \tilde{\overline{H}}_{k,1}^1 + \sum_{m=1}^{2^j} \tilde{\overline{G}}_{m,1}^1 \langle \int_0^x \psi_{j,m}^0, \tilde{\varphi}_{j,k}^1 \rangle. \tag{29}$$

Equations (28) and (29) define two linear systems with respect to the edge scaling function and wavelet filters $\tilde{\overline{G}}_{n,1}^1$ and $\tilde{\overline{H}}_{n,1}^1$. From [2, 20], the computation of coefficients $\langle \int_0^x \psi_{j,m}^0, \tilde{\psi}_{j,k}^1 \rangle$ and $\langle \int_0^x \psi_{j,m}^0, \tilde{\varphi}_{j,k}^1 \rangle$ is straightforward and this is done only for functions whose support intersect the edge function support, due to the compactly support properties of the generators. Then, solving these linear systems, and similar relations at the boundary 1, allows to get the new edge filters. Finally, the main steps of the decomposition algorithm are summarized as:

$$c_{j,1} = c_{j+1,1} \tilde{\overline{H}}_{1,1}^1, \tag{30}$$

$$c_{j,k} = \sum_{n=2}^{\Delta_{j+1}-1} c_{j+1,n} \tilde{H}_{n,k}^{1,0} + c_{j+1,1} \tilde{\overline{H}}_{k,1}^1 + c_{j+1,\Delta_{j+1}} \tilde{\overline{H}}_{k,\Delta_{j+1}}^1, \ 2 \le k \le \Delta_j \tag{31}$$

$$c_{j,\Delta_j} = c_{j+1,\Delta_{j+1}} \tilde{\overline{H}}_{\Delta_j,\Delta_{j+1}}^1, \tag{32}$$

and

$$d_{j,k} = \sum_{n=2}^{\Delta_{j+1}-1} c_{j+1,n} \tilde{G}_{n,k}^{1,0} + c_{j+1,1} \tilde{\overline{G}}_{k,1}^1 + c_{j+1,\Delta_{j+1}} \tilde{\overline{G}}_{k,\Delta_{j+1}}^1, \ 1 \le k \le 2 \tag{33}$$

Remark 2. *Working in $V_j^{1,0} \subset H_0^1(0,1)$ amounts to work directly with $f_{j+1}^{1,0}$. In this case the elementary decomposition step (27) is reduced to the computations of coefficients (31, 33).*

Fast reconstruction algorithm. For $f_{j+1} \in V_{j+1}^1$, let us suppose that we know its projection onto $V_j^1 \oplus \overline{W}_j^1$ in terms of:

$$f_{j+1} = \sum_{k=1}^{\Delta_j^1} c_{j,k}\varphi_{j,k}^1 + \sum_{m=1}^{2^j} d_{j,m} \int_0^x \psi_{j,m}^0,$$

and we want to compute its projection onto V_{j+1}^1 in terms of:

$$f_{j+1} = \sum_{k=1}^{\Delta_{j+1}^1} c_{j+1,k}\varphi_{j+1,k}^1.$$

Setting

$$\sum_{k=1}^{\Delta_j^1} c_{j,k}\varphi_{j,k}^1 = f_j^0 + f_j^{1,0} + f_j^1, \quad \text{with} \quad f_j^0 = c_{j,1}\varphi_{j,1}^1 \quad \text{and} \quad f_j^1 = c_{j,\Delta_j^1}\varphi_{j,\Delta_j^1}^1,$$

it is easy to see that

$$f_j^{1,0} + \sum_{m=1}^{2^j} d_{j,m} \int_0^x \psi_{j,m}^0 \in V_{j+1}^{1,0},$$

thus we get:

$$c_{j+1,k} = \sum_{n=1}^{\Delta_j^1} c_{j,n} H_{n,k}^1 + \sum_{m=1}^{2^j} d_{j,m} \overline{G}_{m,k}^1, \quad 2 \le k \le \Delta_{j+1}^1 - 1,$$

and

$$c_{j+1,1} = \sum_{n=1}^{\Delta_j^1} c_{j,n} H_{n,1}^1, \qquad c_{j+1,\Delta_{j+1}^1} = \sum_{n=1}^{\Delta_j^1} c_{j,n} H_{n,\Delta_{j+1}^1}^1.$$

Remark 3. *Again working in $V_j^{1,0} \subset H_0^1(0,1)$ amounts to work directly with $f_j^{1,0}$ and $f_{j+1}^{1,0}$, assuming that $f_j^0 = 0$ and $f_j^1 = 0$. Using (30,32), we obtain $c_{j+1,1} = 0$ and $c_{j+1,\Delta_{j+1}^1} = 0$.*

5. Numerical examples

We present in this section numerical examples to illustrate the effectiveness and the potential application of this new construction of multiresolution analyses linked by differentiation and integration. We first show the shape of

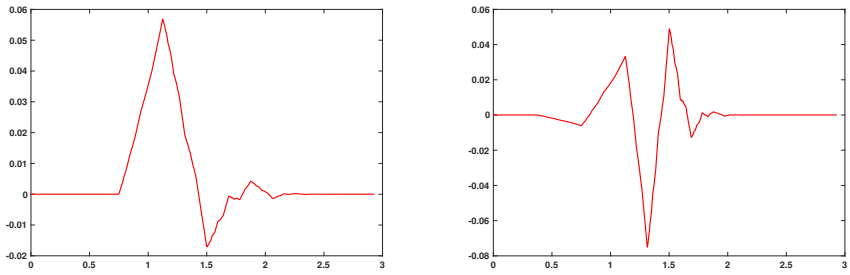

Figure 1: Plot of the internal scaling function φ^0 (left) and the internal wavelet ψ^0 (right). Daubechies orthogonal generator with $r = 3$.

generating functions and study the approximation errors provided by the MRA (V_j^1). Second we apply the new bases to the resolution of a Dirichlet-Laplace problem, only using Fast Wavelet Transforms, leading to a linear complexity for the resolution of the problem.

5.1. Basis functions and approximation errors

For the different examples, the scaling function and wavelet generators (φ^0, ψ^0) considered are Daubechies orthogonal generators, with three vanishing moments for the wavelet [8]. The integer parameters of the construction of V_j^0 thus are:

$$r = 3, \quad \delta_\flat = \delta_\sharp = 1, \quad n_{min} = -r + 1 \quad \text{and} \quad n_{max} = r.$$

On Figure 1, we show the plot of the internal scaling function φ^0 and the wavelet ψ^0. The edge orthogonal scaling functions and wavelets are plotted on Figure 2 and Figure 3 respectively. The generators (φ^1, ψ^1) are computed from (φ^0, ψ^0) using the formula:

$$\varphi^1(x) = \int_{x-1}^{x} \varphi^0(t)dt \qquad \text{and} \qquad \psi^1(x) = 4\int_{-\infty}^{x} \psi^0(t)dt. \tag{34}$$

The graphs of φ^1 and ψ^1 are plotted on Figure 4, Figure 5 and Figure 6 show the plot of the edge scaling function graphs. The edge wavelet graphs are plotted on Figure 7 and Figure 8. We notice that these edge wavelets satisfy homogeneous Dirichlet boundary condition while this boundary condition is not required for

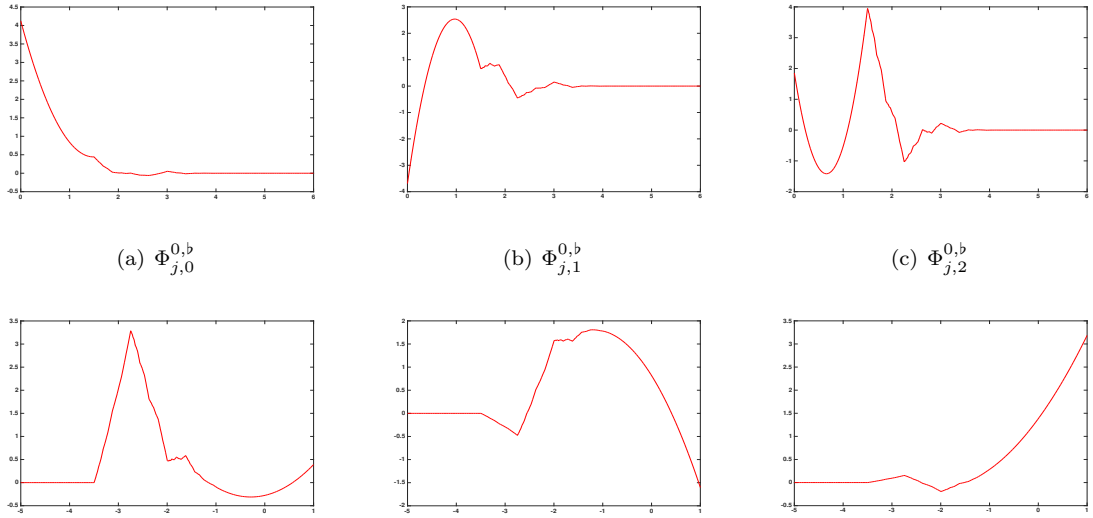

(a) $\Phi_{j,0}^{0,\flat}$ (b) $\Phi_{j,1}^{0,\flat}$ (c) $\Phi_{j,2}^{0,\flat}$

(d) $\Phi_{j,0}^{0,\sharp}$ (e) $\Phi_{j,1}^{0,\sharp}$ (f) $\Phi_{j,2}^{0,\sharp}$

Figure 2: Plot of the edge orthogonal scaling functions of V_j^0. Daubechies orthogonal generator with $r = 3$.

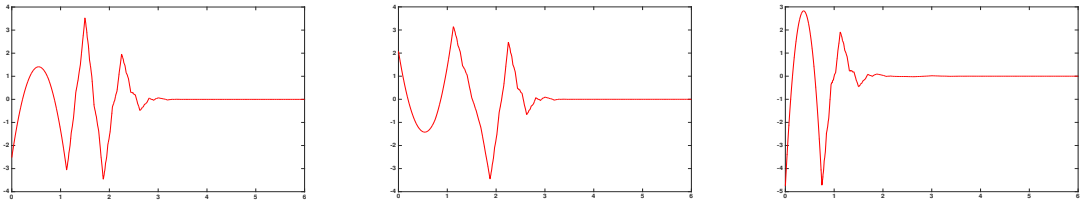

(a) $\Psi_{j,0}^{0,\flat}$ (b) $\Psi_{j,1}^{0,\flat}$ (c) $\Psi_{j,2}^{0,\flat}$

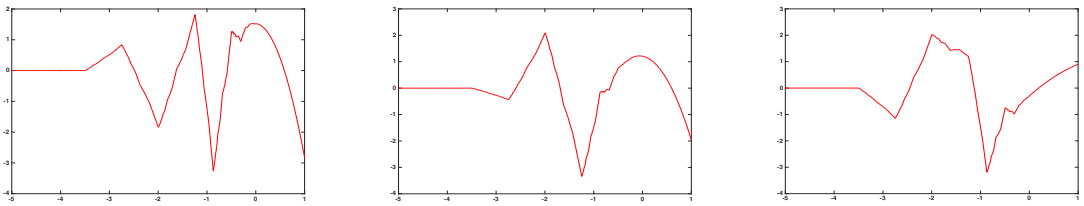

(d) $\Psi_{j,0}^{0,\sharp}$ (e) $\Psi_{j,1}^{0,\sharp}$ (f) $\Psi_{j,2}^{0,\sharp}$

Figure 3: Plot of the edge orthogonal wavelet functions of W_j^0. Daubechies orthogonal generator with $r = 3$.

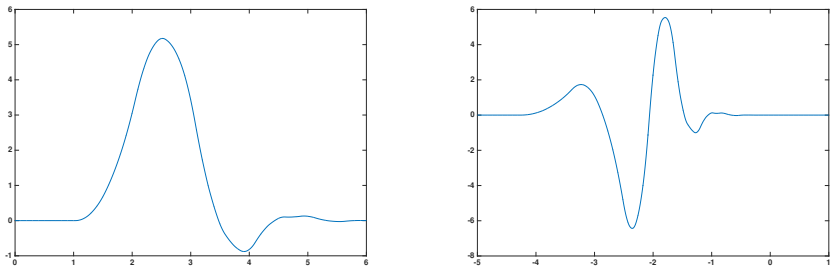

Figure 4: Plot of the internal scaling function $\varphi^1(x) = \int_{x-1}^{x} \varphi^0(t)dt$ (left) and the internal wavelet $\psi^1(x) = 4\int_{-\infty}^{x} \psi^0(t)dt$ (right), where (φ^0, ψ^0) are Daubechies orthogonal generators with $r = 3$.

all the edge scaling functions. Then, to get the multiresolution analysis of $H_0^1(0,1)$ provided by $V_j^{1,0}$, one must remove from V_j^1 the scaling functions $\Phi_{j,0}^{1,\flat}$ and $\Phi_{j,0}^{1,\sharp}$ that allow to reproduce constants at boundaries: this is confirmed again by Figure 5 and Figure 6.

Similarly, the generators $(\tilde{\varphi}^1, \tilde{\psi}^1)$ biorthogonal to (φ^1, ψ^1) are computed using the formula:

$$\varphi^0(x) = \int_x^{x+1} \tilde{\varphi}^1(t)dt \qquad \text{and} \qquad \psi^0(x) = -4\int_{-\infty}^{x} \tilde{\psi}^1(t)dt. \tag{35}$$

The graphs of $\tilde{\varphi}^1$ and $\tilde{\psi}^1$ are plotted on Figure 9, Figure 10 and Figure 11 show the plot of the edge biorthogonal scaling functions. The edge biorthogonal wavelet graphs are plotted on Figure 12 and Figure 13.

We now study the interpolation error of the multiresolution analysis $(V_j^1, \tilde{V}_j^1)$. For a given function f, whose values are known at grid points $x_k = k/2^{j_{max}}$, $0 \le k \le 2^{j_{max}}$, the interpolation step consists of computing its approximation in V_j^1 defined by

$$\mathcal{P}_{j_{max}}^1(f) = \sum_{k=0}^{\Delta_{j_{max}}^1 - 1} < f, \tilde{\varphi}_{j_{max},k}^1 > \varphi_{j_{max},k}^1. \tag{36}$$

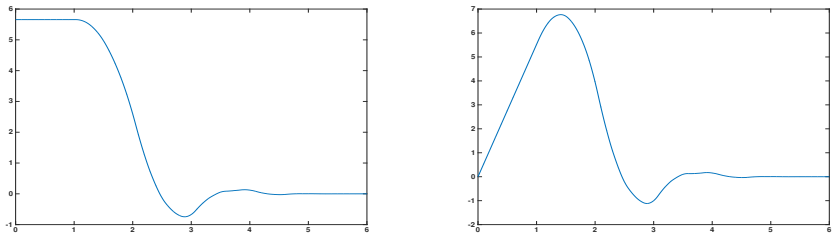

(a) $\Phi^{1,\flat}_{j,0}$ (b) $\Phi^{1,\flat}_{j,1}$

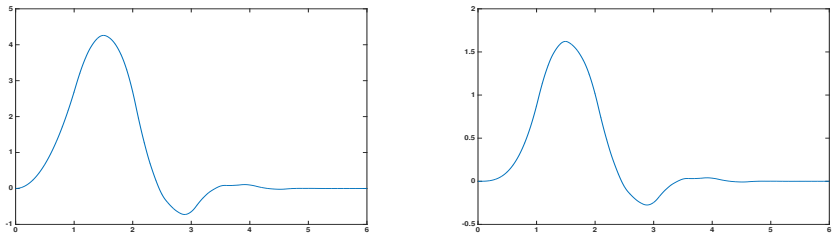

(c) $\Phi^{1,\flat}_{j,2}$ (d) $\Phi^{1,\flat}_{j,3}$

Figure 5: Plot of the edge scaling functions at edge 0, computed from generator $\varphi^1(x) = \int_{x-1}^{x} \varphi^0(t)dt$, where (φ^0, ψ^0) are Daubechies orthogonal generators with $r = 3$.

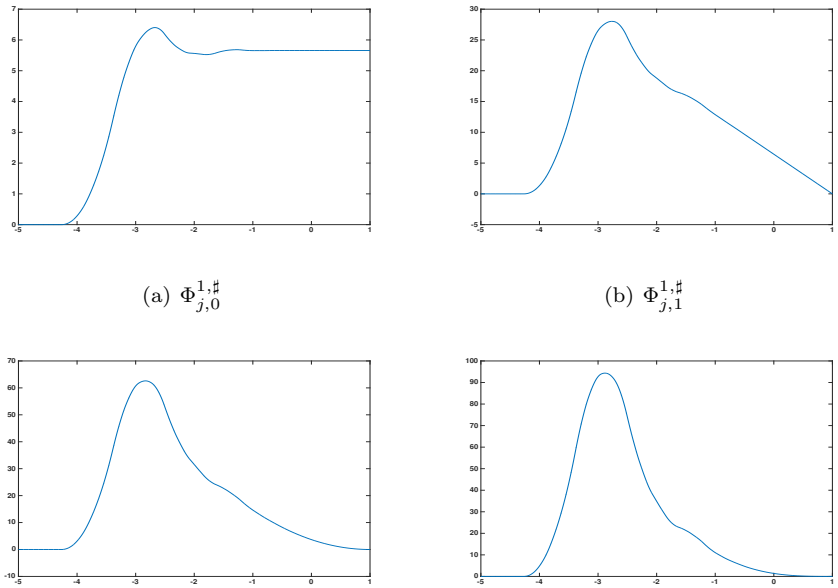

(a) $\Phi_{j,0}^{1,\sharp}$ (b) $\Phi_{j,1}^{1,\sharp}$

(c) $\Phi_{j,2}^{1,\sharp}$ (d) $\Phi_{j,3}^{1,\sharp}$

Figure 6: Plot of the edge scaling functions at edge 1, computed from generator $\varphi^1(x) = \int_{x-1}^{x} \varphi^0(t)dt$, where (φ^0, ψ^0) are Daubechies orthogonal generators with $r = 3$.

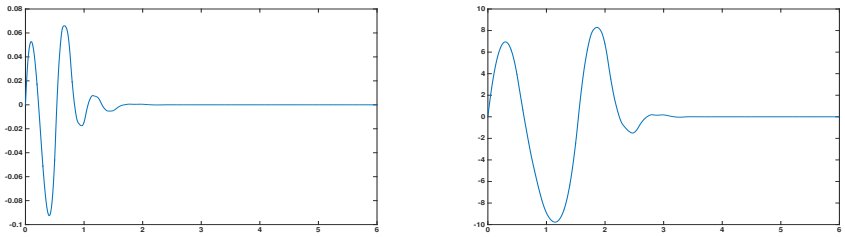

(a) $\Psi^{1,\flat}_{j,0}$ (b) $\Psi^{1,\flat}_{j,1}$

(c) $\Psi^{1,\flat}_{j,2}$ (d) $\Psi^{1,\flat}_{j,3}$

Figure 7: Plot of the edge wavelet at edge 0, computed from generator $\psi^1(x) = 4\int_{-\infty}^{x} \psi^0(t)dt$, where (φ^0, ψ^0) are Daubechies orthogonal generators with $r = 3$.

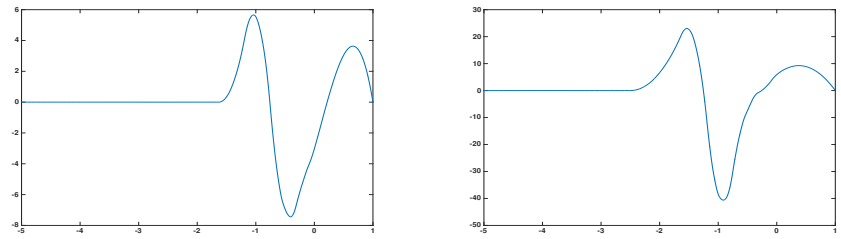

(a) $\Psi_{j,0}^{1,\sharp}$ (b) $\Psi_{j,1}^{1,\sharp}$

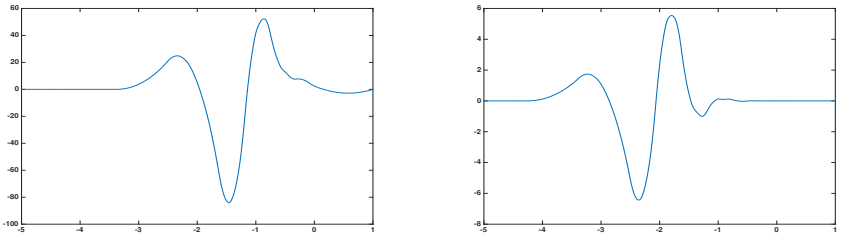

(c) $\Psi_{j,2}^{1,\sharp}$ (d) $\Psi_{j,3}^{1,\sharp}$

Figure 8: Plot of the edge wavelet at edge 1, computed from generator $\psi^1(x) = 4\int_{-\infty}^{x} \psi^0(t)dt$, where (φ^0, ψ^0) are Daubechies orthogonal generators with $r = 3$.

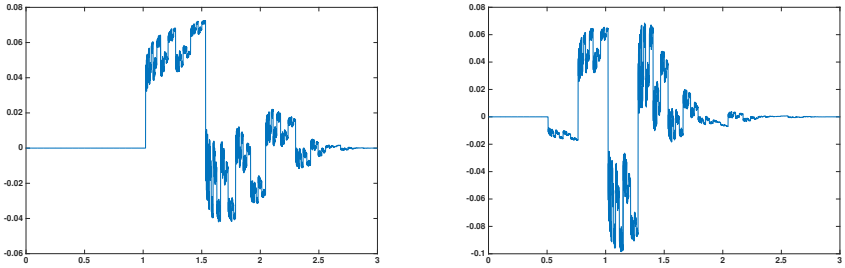

Figure 9: Plot of the internal scaling function $\tilde{\varphi}^1$ (left) and the internal wavelet $\tilde{\psi}^1(t)$ (right), where (φ^0, ψ^0) are Daubechies orthogonal generators with $r = 3$.

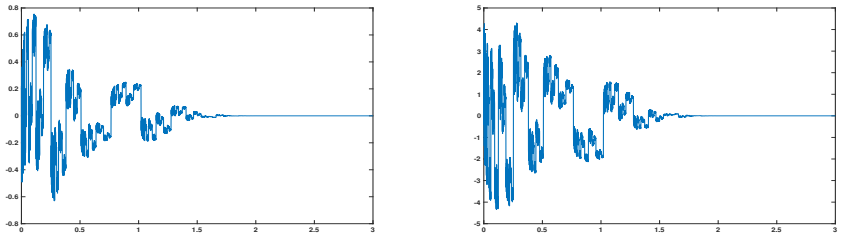

(a) $\tilde{\Phi}^{1,\flat}_{j,0}$ (b) $\tilde{\Phi}^{1,\flat}_{j,1}$

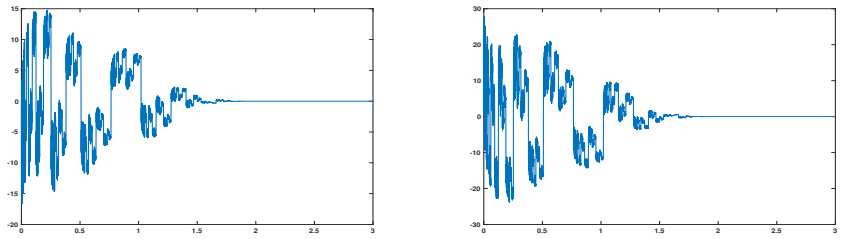

(c) $\tilde{\Phi}^{1,\flat}_{j,2}$ (d) $\tilde{\Phi}^{1,\flat}_{j,3}$

Figure 10: Plot of the edge biorthogonal scaling functions, where (φ^0, ψ^0) are Daubechies orthogonal generators with $r = 3$.

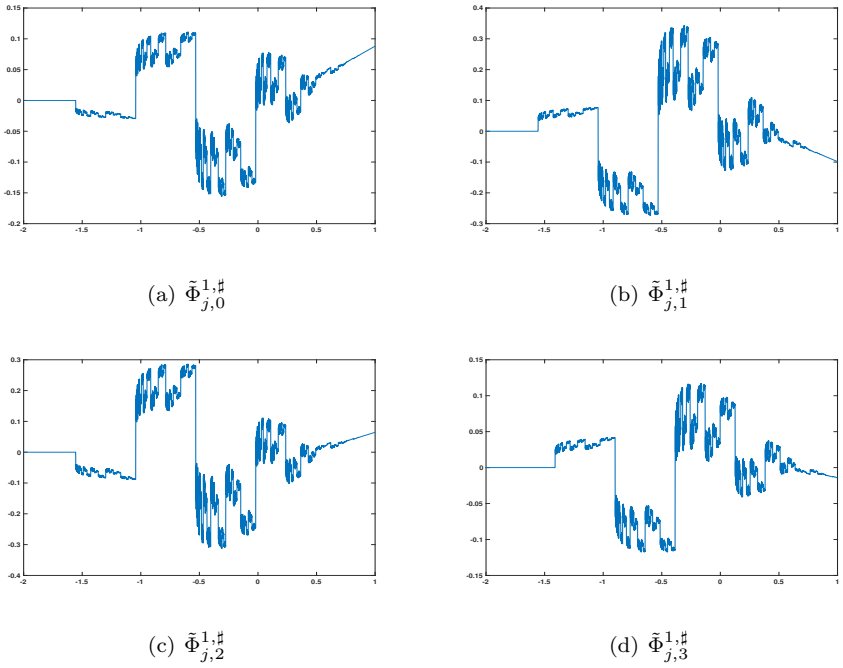

(a) $\tilde{\Phi}^{1,\sharp}_{j,0}$ (b) $\tilde{\Phi}^{1,\sharp}_{j,1}$

(c) $\tilde{\Phi}^{1,\sharp}_{j,2}$ (d) $\tilde{\Phi}^{1,\sharp}_{j,3}$

Figure 11: Plot of the edge biorthogonal scaling functions, where (φ^0, ψ^0) are Daubechies orthogonal generators with $r = 3$.

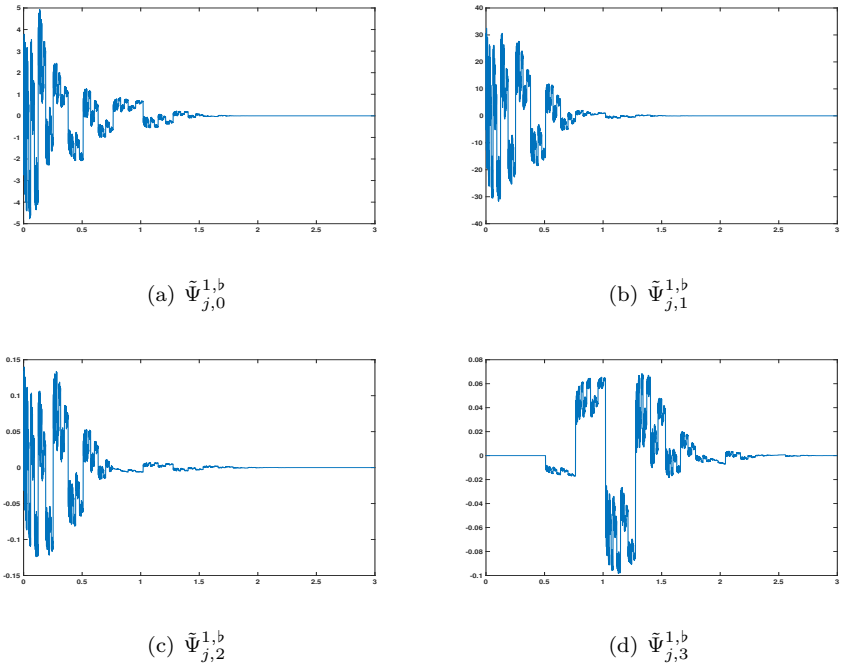

(a) $\tilde{\Psi}^{1,\flat}_{j,0}$ (b) $\tilde{\Psi}^{1,\flat}_{j,1}$

(c) $\tilde{\Psi}^{1,\flat}_{j,2}$ (d) $\tilde{\Psi}^{1,\flat}_{j,3}$

Figure 12: Plot of the edge biorthogonal wavelets, where (φ^0, ψ^0) are Daubechies orthogonal generators with $r = 3$.

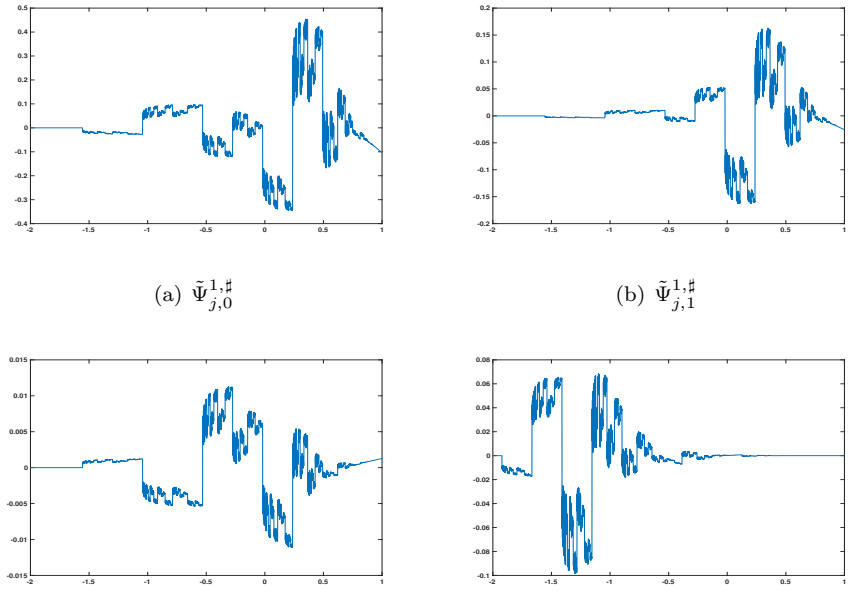

(a) $\tilde{\Psi}^{1,\sharp}_{j,0}$ (b) $\tilde{\Psi}^{1,\sharp}_{j,1}$

(c) $\tilde{\Psi}^{1,\sharp}_{j,2}$ (d) $\tilde{\Psi}^{1,\sharp}_{j,3}$

Figure 13: Plot of the edge biorthogonal wavelets, where (φ^0, ψ^0) are Daubechies orthogonal generators with $r = 3$.

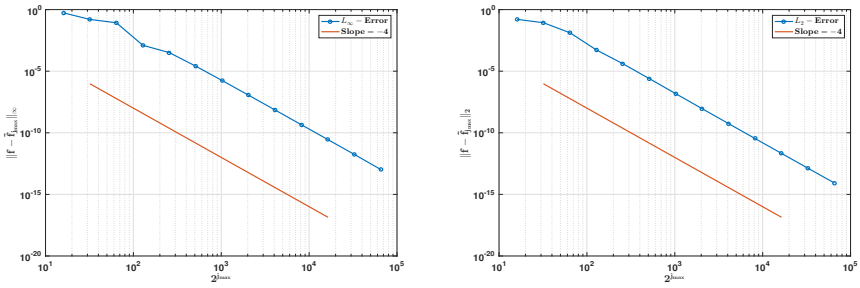

Figure 14: Plot of the interpolation error $\|f - \tilde{f}_{j_{max}}\|_\infty$ (left) and $\|f - \tilde{f}_{j_{max}}\|_2$ (right) in loglog scale, where (φ^0, ψ^0) are Daubechies orthogonal generators with $r = 3$.

We adapted the quadrature formula and algorithms of [16] to the biorthogonal case to compute numerically the inner product $< f, \tilde{\varphi}^1_{j_{max},k} >$. For the function f defined by:

$$f(x) = \sin(2\pi x)\sin(50x) + 1, \tag{37}$$

we show on Figure 14 the snapshot of the interpolation error $\|f - \mathcal{P}^1_{j_{max}}(f)\|$ according to the different values of j_{max}.

Again, from the approximation $\tilde{f}_{j_{max}} = \mathcal{P}^1_{j_{max}}(f)$, we study the projection error in V^1_ℓ:

$$\|\tilde{f}_{j_{max}} - \mathcal{P}^1_\ell(\tilde{f}_{j_{max}})\|, \quad j_{min} \leq \ell \leq j_{max} - 1,$$

involved in the fast wavelet transform algorithm. Figure 15 shows the plot of the projection error in a loglog scale with respect to the resolutions j. The Figure 16 shows the plot of this error at grid points for $j_{max} = 16$ and $j = 9$ or $j = 13$.

To prove the sparse approximation property of the wavelet basis $\psi^1_{j,k}$, we studied the non-linear approximation error of f defined in (37). On Figure 17 we plot the evolution of this error according the ratio of wavelet coefficients retained.

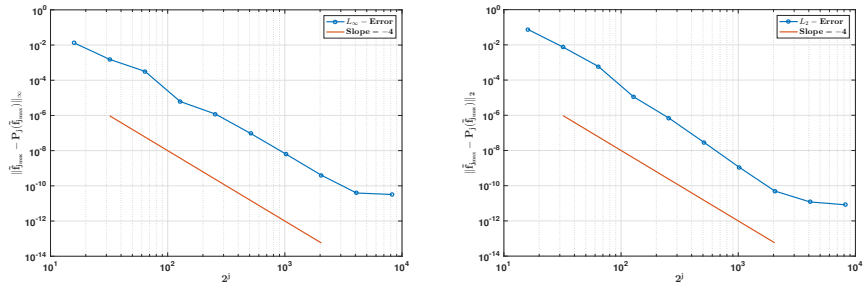

Figure 15: Plot of the projection error $\|\tilde{f}_{j_{max}} - \mathcal{P}^1_\ell(\tilde{f}_{j_{max}})\|_\infty$ (left) and $\|\tilde{f}_{j_{max}} - \mathcal{P}^1_\ell(\tilde{f}_{j_{max}})\|_2$ (right) in loglog scale, where (φ^0, ψ^0) are Daubechies orthogonal generators with $r = 3$

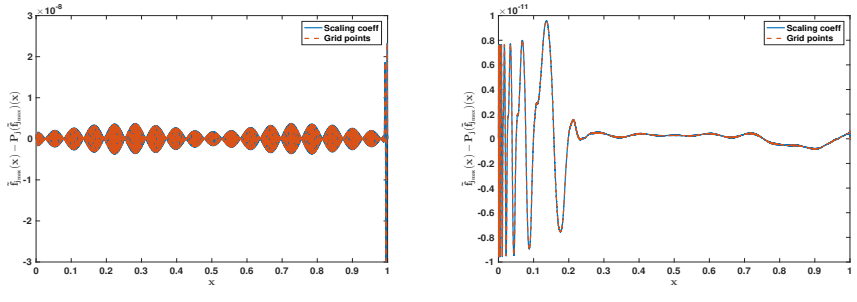

Figure 16: Plot of the projection error $\tilde{f}_{j_{max}} - \mathcal{P}^1_\ell(\tilde{f}_{j_{max}})$ at grid points for $j_{max} = 16$ and $j = 9$ (left) and for $j = 13$ (right), where (φ^0, ψ^0) are Daubechies orthogonal generators with $r = 3$.

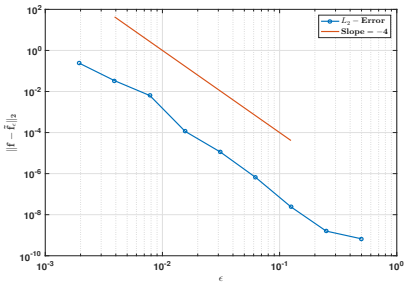

Figure 17: Plot of the non linear approximation L_2-errror. Daubechies orthogonal generator with $r = 3$.

In each of these experiences, the errors decay order obtained is about $s \approx -4$. Since f is very smooth, this is in accordance with the theoretical order which is the polynomial approximation order of the space V_j^1.

5.2. One dimensional laplacian operator

In this section, we evaluate the performance of our new wavelet basis construction, in the numerical resolution of one dimensional Poisson equation with homogeneous Dirichlet boundary condition:

$$\begin{cases} -u''(x) = f(x), \quad x \in]0,1[, \\ \\ u(0) = u(1) = 0. \end{cases} \tag{38}$$

Usually, the numerical resolution of problem (38) with a wavelet based method is done using a Galerkin (or Petrov-Galerkin) method. This leads to the resolution of a linear algebraic system with the stiffness matrix of the considered wavelet basis [2, 6]. In our construction, the wavelet basis $\psi_{j,k}^0$ can be chosen as an orthogonal basis. In this case, it is easy to see that the stiffness matrix of the wavelet basis $\psi_{j,k}^1$ constructed by integrating $\psi_{j,k}^0$ is a diagonal matrix:

$$< -(\psi_{j,k}^1)'', \psi_{\ell,n}^1 >=< (\psi_{j,k}^1)', (\psi_{\ell,n}^1)' >= 2^{j+\ell} < \psi_{j,k}^0, \psi_{\ell,n}^0 >= 2^{j+\ell}\delta_{j,\ell}\delta_{k,n}. \tag{39}$$

Then, if the solution u is searched in terms of its wavelet series:

$$u = \sum_{j,k} u_{j,k}\psi_{j,k}^1, \tag{40}$$

the coefficients $u_{j,k}$ are given by:

$$u_{j,k} = 2^{-2j-4} f_{j,k}, \quad \text{where} \quad f = \sum_{j,k} f_{j,k}\tilde{\psi}_{j,k}^1. \tag{41}$$

Thus, the resolution of (38) is reduced to a wavelet coefficient normalization, with a linear numerical complexity. We notice that, at the coarse scale j_{min} we also have to invert the stiffness matrix of the scaling function $\varphi_{j_{min},k}^1$. The size of this matrix is very small compared to the size of the whole system.

To see the efficiency of this approach, we firstly compare its numerical complexity to the complexity of a finite difference method and the multi-grid method of [12]. The main criterion we took is the real computational time of the MATLAB code [17] that encodes the method. For this purpose, two numerical experiences have been conducted. The first experience is done with the exact solution:

$$u(x) = x^3 - x^4. \tag{42}$$

The source term f is appropriately computed from the solution u. On Tab. 1, we provide the different mean real computational time according to the space resolution j. It can be observed that the present method performs better than these two methods when the resolution j increases, with a good accuracy on the relative L_2-error.

Computational time			
Method	resolution j	t (seconds)	L_2-error
Multi-grid	8	0.010705	$4.4184E^{-5}$
Present	8	0.000625	$1.3302E^{-9}$
Finite difference	8	0.000205	$4.4341E^{-5}$
Multi-grid	10	0.019202	$2.7255E^{-6}$
Present	10	0.000835	$3.1552E^{-11}$
Finite difference	10	0.000389	$2.7640E^{-6}$
Multi-grid	16	0.089770	$2.0575E^{-7}$
Present	16	0.007712	$5.6942E^{-11}$
Finite difference	16	0.018695	$9.2095E^{-10}$

Table 1: Comparison of the real computational time and the relative L^2-error for the exact solution: $u(x) = x^3 - x^4$.

The second experience concerns the source term f defined by:

$$f(x) = \begin{cases} 0, & 0 \leq x < 3/8, \\ 2, & 3/8 \leq x \leq 5/8, \\ 0, & 5/8 < x \leq 1, \end{cases} \tag{43}$$

and this corresponds to an exact solution u of (38) defined by:

$$u(x) = \begin{cases} \frac{1}{4}x, & 0 \leq x < 3/8, \\ -x^2 + x - \frac{9}{64}, & 3/8 \leq x \leq 5/8, \\ -\frac{1}{4}x + \frac{1}{4}, & 5/8 < x \leq 1. \end{cases} \tag{44}$$

The function f has discontinuities at $x = 3/8$ and $x = 5/8$. Then, the motivation for this experience is to highlight the adaptativity of the wavelet basis $\psi^1_{j,k}$.

6. Fast divergence-free wavelet transform

Another application of our new construction of wavelet linked by differentiation and integration is the implementation of a fast divergence-free wavelet transform algorithm, similar to this of [9] for the periodic case. Since we have a diagonal differentiation relation between the wavelets $\psi^{1,0}_{j,k}$ and $\psi^0_{j,k}$ even at boundaries, the algorithm will be the same, except that we have to take care of the lowest scale j_{min}, which cannot be equal to 0 as in the periodic case. To make the text simpler, we will present only the three dimensional case, knowing that the generalization to higher dimension is straightforward.

Specifically, the divergence-free function space that we are concerned is $\mathcal{H}_{div}(\Omega)$:

$$\mathcal{H}_{div}(\Omega) = \{\boldsymbol{u} \in (L^2(\Omega))^3 : \ \nabla \cdot \boldsymbol{u} = 0 \text{ and } \boldsymbol{u} \cdot \vec{\boldsymbol{n}}|_{\partial\Omega} = 0\}, \tag{45}$$

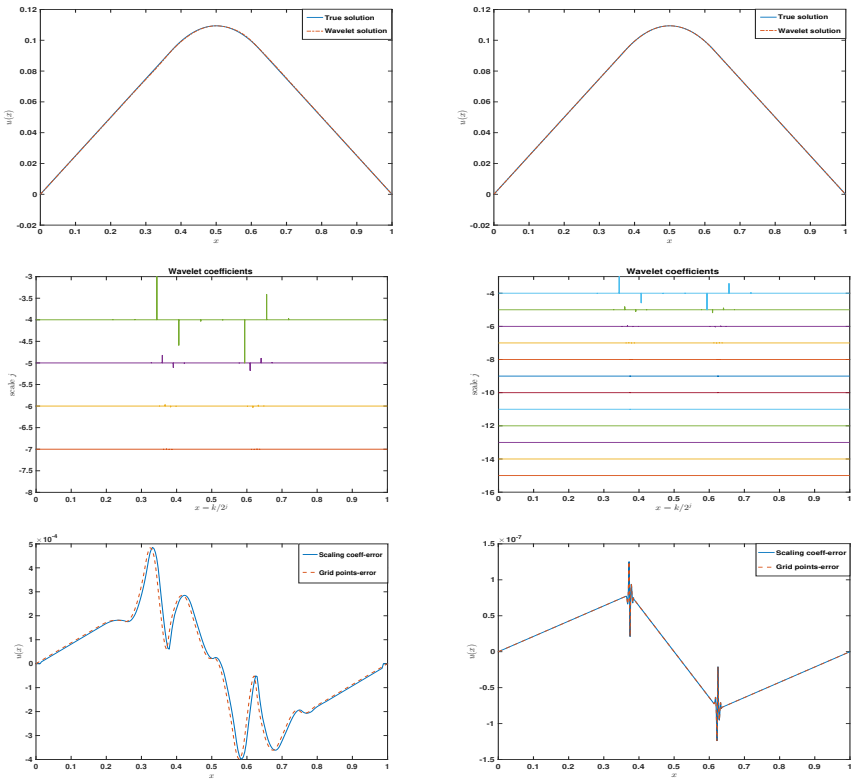

Figure 18: From top to bottom, plot of the computed solution, its wavelet coefficients and the residual error (first column $j = 8$ and second column $j = 16$). Where (φ^0, ψ^0) are Daubechies orthogonal generators with $r = 3$.

where $\Omega = [0,1]^3$ and $\vec{\boldsymbol{n}}$ denotes the unit outward normal at boundary $\partial\Omega$.

For the sake of convenience, we denote by $\{\psi^{1,0}_{j,k}\}$ and $\{\psi^{0}_{j,k}\}$ the scaling functions and wavelets of $V^{1,0}_j$ and V^0_j, respectively (the scaling function at coarsest scale j_{min} will be denoted like the wavelet but with a scale index $j = j_{min} - 1$). In the three dimensional case, as explained in [9, 20, 21, 22, 23] one can construct three kind of anisotropic divergence-free wavelets by:

$$\Psi^{div,1}_{\boldsymbol{j},\boldsymbol{k}} := \mathbf{curl} \begin{vmatrix} 0 \\ 0 \\ \psi^{1,0}_{j_1,k_1} \otimes \psi^{1,0}_{j_2,k_2} \otimes \psi^{0}_{j_3,k_3} \end{vmatrix} = \begin{vmatrix} \psi^{1,0}_{j_1,k_1} \otimes (\psi^{1,0}_{j_2,k_2})' \otimes \psi^{0}_{j_3,k_3} \\ -(\psi^{1,0}_{j_1,k_1})' \otimes \psi^{1,0}_{j_2,k_2} \otimes \psi^{0}_{j_3,k_3} \\ 0 \end{vmatrix}, \tag{46}$$

$$\Psi^{div,2}_{\boldsymbol{j},\boldsymbol{k}} := \mathbf{curl} \begin{vmatrix} \psi^{0}_{j_1,k_1} \otimes \psi^{1,0}_{j_2,k_2} \otimes \psi^{1,0}_{j_3,k_3} \\ 0 \\ 0 \end{vmatrix} = \begin{vmatrix} 0 \\ \psi^{0}_{j_1,k_1} \otimes \psi^{1,0}_{j_2,k_2} \otimes (\psi^{1,0}_{j_3,k_3})' \\ -\psi^{0}_{j_1,k_1} \otimes (\psi^{1,0}_{j_2,k_2})' \otimes \psi^{1,0}_{j_3,k_3} \end{vmatrix}, \tag{47}$$

$$\Psi^{div,3}_{\boldsymbol{j},\boldsymbol{k}} := \mathbf{curl} \begin{vmatrix} 0 \\ \psi^{1,0}_{j_1,k_1} \otimes \psi^{0}_{j_2,k_2} \otimes \psi^{1,0}_{j_3,k_3} \\ 0 \end{vmatrix} = \begin{vmatrix} -\psi^{1,0}_{j_1,k_1} \otimes \psi^{0}_{j_2,k_2} \otimes (\psi^{1,0}_{j_3,k_3})' \\ 0 \\ (\psi^{1,0}_{j_1,k_1})' \otimes \psi^{0}_{j_2,k_2} \otimes \psi^{1,0}_{j_3,k_3} \end{vmatrix}, \tag{48}$$

By construction these wavelets are contained in $\mathcal{H}_{div}(\Omega)$ and the space $\mathbf{W}^{div}_{\boldsymbol{j}}$ that they spanned is included into the BMRA of $(L^2(\Omega))^3$ endowed with the free-slip boundary condition generated by:

$$\vec{\mathbf{V}}_j = \left(V^{1,0}_j \otimes V^0_j \otimes V^0_j\right) \times \left(V^0_j \otimes V^{1,0}_j \otimes V^0_j\right) \times \left(V^0_j \otimes V^0_j \otimes V^{1,0}_j\right). \tag{49}$$

According to Proposition 7, the spaces $\vec{\mathbf{V}}_j$ provide an internal multiscale approximation process for $\mathcal{H}_{div}(\Omega)$. Precisely, let $\vec{\mathbf{P}}_j$ be the biorthogonal multiscale projector associated to $\vec{\mathbf{V}}_j$:

$$\vec{\mathbf{P}}_j = \left(\mathcal{P}^{1,0}_j \otimes \mathcal{P}^0_j \otimes \mathcal{P}^0_j\right) \times \left(\mathcal{P}^0_j \otimes \mathcal{P}^{1,0}_j \otimes \mathcal{P}^0_j\right) \times \left(\mathcal{P}^0_j \otimes \mathcal{P}^0_j \otimes \mathcal{P}^{1,0}_j\right),$$

and $\mathbf{P}_j^0 = \mathcal{P}_j^0 \otimes \mathcal{P}_j^0 \otimes \mathcal{P}_j^0$ the projector associated to $\mathbf{V}_j^0 = V_j^0 \otimes V_j^0 \otimes V_j^0$. Then, the commutation of the one dimensional multiscale projectors with differentiation allows to get:

$$\forall\ \boldsymbol{u} \in \mathcal{H}_{div}(\Omega),\ \nabla \cdot \vec{\mathbf{P}}_j(\boldsymbol{u}) = \mathbf{P}_j^0(\nabla \cdot \boldsymbol{u}) = 0\ \Rightarrow\ \vec{\mathbf{P}}_j(\mathcal{H}_{div}(\Omega)) = \vec{\mathbf{V}}_j \cap \mathcal{H}_{div}(\Omega).$$

Thus, the spaces $\vec{\mathbf{V}}_j^{div} = \vec{\mathbf{V}}_j \cap \mathcal{H}_{div}(\Omega)$ constitute a multiresolution analysis of $\mathcal{H}_{div}(\Omega)$ and the anisotropic multiscale decomposition of $\vec{\mathbf{V}}_j^{div}$ reads:

$$\vec{\mathbf{V}}_j^{div} = \vec{\mathbf{V}}_{j_{min}}^{div} \bigoplus_{j_{min} \le |\boldsymbol{j}| \le j-1} \mathbf{W}_{\boldsymbol{j}}^{div}.$$

Proposition 8. *A basis of the finite dimensional space $\vec{\mathbf{V}}_j^{div} = \vec{\mathbf{V}}_j \cap \mathcal{H}_{div}(\Omega)$ is given by the following divergence-free scaling function basis:*

$$\vec{\mathbf{V}}_j^{div} = span\{\Phi_{j,\boldsymbol{k}}^{div,1}, \Phi_{j,\boldsymbol{k}}^{div,2}\}, \tag{50}$$

where

$$\Phi_{j,\boldsymbol{k}}^{div,1} := \mathbf{curl} \begin{vmatrix} 0 \\ 0 \\ \varphi_{j,k_1}^{1,0} \otimes \varphi_{j,k_2}^{1,0} \otimes \varphi_{j,k_3}^{0} \end{vmatrix} = \begin{vmatrix} \varphi_{j_1,k_1}^{1,0} \otimes (\varphi_{j_2,k_2}^{1,0})' \otimes \varphi_{j_3,k_3}^{0} \\ -(\varphi_{j_1,k_1}^{1,0})' \otimes \varphi_{j_2,k_2}^{1,0} \otimes \varphi_{j_3,k_3}^{0} \\ 0 \end{vmatrix}, \tag{51}$$

and

$$\Phi_{j,\boldsymbol{k}}^{div,2} := \mathbf{curl} \begin{vmatrix} \varphi_{j,k_1}^{0} \otimes \varphi_{j,k_2}^{1,0} \otimes \varphi_{j,k_3}^{1,0} \\ 0 \\ 0 \end{vmatrix} = \begin{vmatrix} 0 \\ \varphi_{j_1,k_1}^{0} \otimes \varphi_{j_2,k_2}^{1,0} \otimes (\varphi_{j_3,k_3}^{1,0})' \\ -\varphi_{j_1,k_1}^{0} \otimes (\varphi_{j_2,k_2}^{1,0})' \otimes \varphi_{j_3,k_3}^{1,0} \end{vmatrix}, \tag{52}$$

294 *with $2 \le k_1, k_2 \le \Delta_j^1 - 1$ and $1 \le k_3 \le \Delta_j^0 - 1$ for $\Phi_{j,\boldsymbol{k}}^{div,1}$ and $2 \le k_2, k_3 \le \Delta_j^1 - 1$*
295 *and $1 \le k_1 \le \Delta_j^0 - 1$ for $\Phi_{j,\boldsymbol{k}}^{div,2}$.*

296

Proof. First by construction we have $span\{\Phi_{j,\boldsymbol{k}}^{div,1}, \Phi_{j,\boldsymbol{k}}^{div,2}\} \subset \vec{\mathbf{V}}_j^{div}$, using (26) left which leads to:

$$(\varphi_{j,k}^{1,0})' = \sum_{n=1}^{\Delta_j^1 - 1} (L_j^{1,0})_{k,n}\ \varphi_{j,n}^{0}$$

This shows the first inclusion.

Conversely, let $\boldsymbol{u} \in \vec{\mathbf{V}}_j^{div}$ and denote by $c^1_{\boldsymbol{k}}$, $c^2_{\boldsymbol{k}}$ and $c^3_{\boldsymbol{k}}$ the coefficients of its decomposition onto the scaling function basis of $\vec{\mathbf{V}}_j$:

$$\boldsymbol{u} = \left(\sum_{\boldsymbol{k}} c^1_{\boldsymbol{k}} \phi^1_{j,\boldsymbol{k}}; \sum_{\boldsymbol{k}} c^2_{\boldsymbol{k}} \phi^2_{j,\boldsymbol{k}}; \sum_{\boldsymbol{k}} c^3_{\boldsymbol{k}} \phi^3_{j,\boldsymbol{k}} \right),$$

where $\phi^1_{j,\boldsymbol{k}} := \varphi^{1,0}_{j,k_1} \otimes \varphi^0_{j,k_2} \otimes \varphi^0_{j,k_3}$, $\phi^2_{j,\boldsymbol{k}} := \varphi^0_{j,k_1} \otimes \varphi^{1,0}_{j,k_2} \otimes \varphi^0_{j,k_3}$ and $\phi^3_{j,\boldsymbol{k}} := \varphi^0_{j,k_1} \otimes \varphi^0_{j,k_2} \otimes \varphi^{1,0}_{j,k_3}$.

Now, from $\boldsymbol{u}$ we define a divergence-free function $\boldsymbol{u}^{div} \in span\{\Phi^{div,1}_{j,\boldsymbol{k}}, \Phi^{div,2}_{j,\boldsymbol{k}}\}$ by:

$$\boldsymbol{u}^{div} = \sum_{\boldsymbol{k}} c^{div,1}_{\boldsymbol{k}} \Phi^{div,1}_{j,\boldsymbol{k}} + \sum_{\boldsymbol{k}} c^{div,2}_{\boldsymbol{k}} \Phi^{div,2}_{j,\boldsymbol{k}},$$

with

$$c^{div,1}_{k_1,k_2,k_3} = \langle \sum_{\boldsymbol{m}} c^1_{\boldsymbol{m}} \phi^1_{j,\boldsymbol{m}}, -\tilde{\varphi}^{1,0}_{j,k_1} \otimes \int_0^x \tilde{\varphi}^{1,0}_{j,k_2} \otimes \tilde{\varphi}^0_{j,k_3} \rangle = -\sum_m c^1_{k_1,m,k_3} (\widetilde{L}^{1,0}_j)_{k_2,m}$$

and

$$c^{div,2}_{k_1,k_2,k_3} = \langle \sum_{\boldsymbol{m}} c^3_{\boldsymbol{m}} \phi^3_{j,\boldsymbol{m}}, \tilde{\varphi}^0_{j,k_1} \otimes \int_0^x \tilde{\varphi}^{1,0}_{j,k_2} \otimes \tilde{\varphi}^{1,0}_{j,k_3} \rangle = \sum_m c^3_{k_1,m,k_3} (\widetilde{L}^{1,0}_j)_{k_2,m},$$

where $L^{1,0}_j$ and $\widetilde{L}^{1,0}_j$ are the change of bases matrices defined in (26). Then, to get the second inclusion $\vec{\mathbf{V}}_j^{div} \subset \ span\{\Phi^{div,1}_{j,\boldsymbol{k}}, \Phi^{div,2}_{j,\boldsymbol{k}}\}$, it suffices to prove that $\boldsymbol{u} - \boldsymbol{u}^{div} = 0$.

For this, let $\bar{c}^1_{\boldsymbol{k}}$, $\bar{c}^2_{\boldsymbol{k}}$ and $\bar{c}^3_{\boldsymbol{k}}$ be the coefficients of the decomposition of $\boldsymbol{u}^{div}$ onto the scaling function basis of $\vec{\mathbf{V}}_j$. Since the following biorthogonal relation holds:

$$\langle (\varphi^{1,0}_{j,k})', -\int_0^x \tilde{\varphi}^{1,0}_{j,n} \rangle = \langle \varphi^{1,0}_{j,k}, \tilde{\varphi}^{1,0}_{j,n} \rangle = -(L^{1,0}_j \ {}^t\widetilde{L}^{1,0}_j)_{n,k} = \delta_{n,k}, \tag{53}$$

a simple computation shows that:

$$\bar{c}^1_{\boldsymbol{k}} = c^1_{\boldsymbol{k}}, \quad \bar{c}^2_{\boldsymbol{k}} = \sum_m \left(-c^{div,1}_{m,k_2,k_3} (L^{1,0}_j)_{m,k_1} + c^{div,2}_{k_1,k_2,m} (L^{1,0}_j)_{m,k_3} \right) \quad \text{and} \quad \bar{c}^3_{\boldsymbol{k}} = c^3_{\boldsymbol{k}}.$$

On the other hand, the divergence-free relation $\nabla \cdot \boldsymbol{u} = 0$ expressed in terms of the coefficients $c^1_{\boldsymbol{k}}$, $c^2_{\boldsymbol{k}}$ and $c^3_{\boldsymbol{k}}$ reads:

$$\sum_m \left(c^1_{m,k_2,k_3} (L^{1,0}_j)_{m,k_1} + c^2_{k_1,m,k_3} (L^{1,0}_j)_{m,k_2} + c^3_{k_1,k_2,m} (L^{1,0}_j)_{m,k_3} \right) = 0.$$

300 Then, using again the relation (53) we get:

$$\begin{aligned} c^2_{k_1,k_2,k_3} &= -\sum_n \sum_m \left(c^1_{m,n,k_3} (L_j^{1,0})_{m,k_1} (\widetilde{L}_j^{1,0})_{k_2,n} + c^3_{k_1,n,m} (L_j^{1,0})_{m,k_3} (\widetilde{L}_j^{1,0})_{k_2,n} \right) \\ &= \sum_m \left([\sum_n c^1_{m,n,k_3} (\widetilde{L}_j^{1,0})_{k_2,n}] (L_j^{1,0})_{m,k_1} + [\sum_n c^3_{k_1,n,m} (\widetilde{L}_j^{1,0})_{k_2,n}] (L_j^{1,0})_{m,k_3} \right) \\ &= \sum_m \left(-c^{div,1}_{m,k_2,k_3} (L_j^{1,0})_{m,k_1} + c^{div,2}_{k_1,k_2,m} (L_j^{1,0})_{m,k_3} \right). \end{aligned}$$

301 Thus $\vec{c}^2_{\boldsymbol{k}} = c^2_{\boldsymbol{k}}$, which means that $\boldsymbol{u} - \boldsymbol{u}^{div} = 0$. □

302

This proposition provides an algorithm that allows us to compute $c^{div,1}_{\boldsymbol{k}}$ and $c^{div,2}_{\boldsymbol{k}}$ from $c^1_{\boldsymbol{k}}$, $c^2_{\boldsymbol{k}}$ and $c^3_{\boldsymbol{k}}$ by:

$$c^{div,1}_{k_1,k_2,k_3} = -\sum_m c^1_{k_1,m,k_3} (\widetilde{L}_j^{1,0})_{k_2,m} \quad \text{and} \quad c^{div,2}_{k_1,k_2,k_3} = \sum_m c^3_{k_1,m,k_3} (\widetilde{L}_j^{1,0})_{k_2,m}. \tag{54}$$

303 Conversely, from $c^{div,1}_{\boldsymbol{k}}$ and $c^{div,2}_{\boldsymbol{k}}$ one can compute $c^1_{\boldsymbol{k}}$, $c^2_{\boldsymbol{k}}$ and $c^3_{\boldsymbol{k}}$ by:

$$c^1_{k_1,k_2,k_3} = \sum_m c^{div,1}_{k_1,m,k_3} (L_j^{1,0})_{m,k_2} \tag{55}$$

$$c^2_{k_1,k_2,k_3} = \sum_m \left(-c^{div,1}_{m,k_2,k_3} (L_j^{1,0})_{m,k_1} + c^{div,2}_{k_1,k_2,m} (L_j^{1,0})_{m,k_3} \right) \tag{56}$$

$$c^3_{k_1,k_2,k_3} = -\sum_m c^{div,2}_{k_1,m,k_3} (L_j^{1,0})_{m,k_2}. \tag{57}$$

On the wavelet basis, this change of bases reduces to a simple wavelet coefficients renormalization as in the periodic case: let $d^1_{\boldsymbol{j},\boldsymbol{k}}$, $d^2_{\boldsymbol{j},\boldsymbol{k}}$ and $d^3_{\boldsymbol{j},\boldsymbol{k}}$ be the coefficients of the decomposition of $\boldsymbol{u}$ in the anisotropic wavelet basis associated to $\vec{\mathbf{V}}_j$, and $d^{div,1}_{\boldsymbol{j},\boldsymbol{k}}$ and $d^{div,2}_{\boldsymbol{j},\boldsymbol{k}}$ the coefficients of its decomposition in the wavelet basis of $\vec{\mathbf{W}}^{div}_j$. Then, we have:

$$d^{div,1}_{\boldsymbol{j},\boldsymbol{k}} = 2^{-j_2-2} d^1_{\boldsymbol{j},\boldsymbol{k}} \quad \text{and} \quad d^{div,2}_{\boldsymbol{j},\boldsymbol{k}} = -2^{-j_2-2} d^3_{\boldsymbol{j},\boldsymbol{k}}, \tag{58}$$

and

$$d^1_{\boldsymbol{j},\boldsymbol{k}} = 2^{j_2+2} d^{div,1}_{\boldsymbol{j},\boldsymbol{k}}, \quad d^2_{\boldsymbol{j},\boldsymbol{k}} = -2^{j_1+2} d^{div,1}_{\boldsymbol{j},\boldsymbol{k}} + 2^{j_3+2} d^{div,2}_{\boldsymbol{j},\boldsymbol{k}} \quad \text{and} \quad d^3_{\boldsymbol{j},\boldsymbol{k}} = -2^{j_2+2} d^{div,2}_{\boldsymbol{j},\boldsymbol{k}}. \tag{59}$$

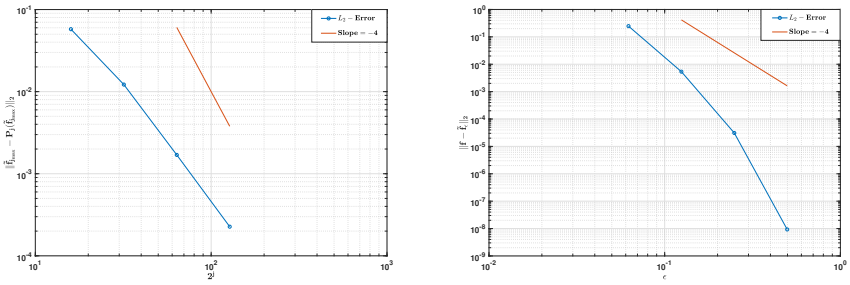

Figure 19: Linear approximation L^2-error (left) and nonlinear approximation L^2-error (right) in log-log scale, obtained with the fast divergence-free transform algorithm. Where $\boldsymbol{u}$ is defined in (60) and (φ^0, ψ^0) are Daubechies orthogonal generators with $r = 3$.

Remark 4.

As no distinction is made between the scaling functions $\varphi^{1,0}_{j,k}$ and the wavelet $\psi^{1,0}_{j,k}$ in the definition of the divergence-free wavelets (46, 47, 48), the definition of coefficients $(d^{div,1}_{\boldsymbol{j},\boldsymbol{k}}, d^{div,2}_{\boldsymbol{j},\boldsymbol{k}})$ and $(c^1_{\boldsymbol{j},\boldsymbol{k}}, c^2_{\boldsymbol{j},\boldsymbol{k}}, c^3_{\boldsymbol{j},\boldsymbol{k}})$ in (58, 59) must be adapted following the scaling function cases listed above if at least one coordinate of $\boldsymbol{j}$ is j_{min}.

We tested the fast divergence-free wavelet transform algorithm on a toy vector field $\boldsymbol{u}$ defined by:

$$\boldsymbol{u}(x,y,z) = \begin{vmatrix} \sin^2(2\pi x)\sin(4\pi y)\sin(4\pi z) \\ \sin(4\pi x)\sin^2(2\pi y)\sin(4\pi z) \\ -2\sin(4\pi x)\sin(4\pi y)\sin^2(2\pi z) \end{vmatrix} \tag{60}$$

For the construction of $V^{1,0}_j$ and V^0_j, we kept the same parameters as in the previous sections: again (φ^0, ψ^0) are the Daubechies orthogonal generators with $r = 3$. On Figure 19, we show both the plot of the linear and nonlinear approximation L^2-errors in a log-log scale. Since the vector field $\boldsymbol{u}$ is smooth enough, the expected decay orders of the errors are achieved.

The construction extends to larger dimensions $d > 3$ readily. We obtain in this case $(d-1)$ types of linear independent divergence-free wavelet functions. For $1 \leq i \leq d-1$, the general formula of these wavelets is given by:

$$\Psi^{div,i}_{\boldsymbol{j},\boldsymbol{k}} := \begin{array}{c|l} & 0 \\ & \vdots \\ & 0 \\ \text{row } i & 2^{j_{i+1}+2}\psi^0_{j_1,k_1} \otimes \cdots \otimes \psi^0_{j_{i-1},k_{i-1}} \otimes \psi^{1,0}_{j_i,k_i} \otimes \psi^0_{j_{i+1},k_{i+1}} \otimes \cdots \otimes \psi^0_{j_d,k_d} \\ \text{row } i+1 & -2^{j_i+2}\psi^0_{j_1,k_1} \otimes \cdots \otimes \psi^0_{j_i,k_i} \otimes \psi^{1,0}_{j_{i+1},k_{i+1}} \otimes \psi^0_{j_{i+1},k_{i+2}} \otimes \cdots \otimes \psi^0_{j_d,k_d} \\ & 0 \\ & \vdots \\ & 0 \end{array} \tag{61}$$

The wavelets $\Psi^{div,i}_{\boldsymbol{j},\boldsymbol{k}}$ satisfy the boundary condition $\Psi^{div,i}_{\boldsymbol{j},\boldsymbol{k}} \cdot \vec{\boldsymbol{n}} = 0$ by construction. The space $\mathbf{W}^{div}_{\boldsymbol{j}}$ spanned by these wavelets is included into the following standard BMRA of $(L^2(\Omega))^d$:

$$\vec{\mathbf{V}}_j = \mathbf{V}^1_j \times \cdots \times \mathbf{V}^d_j \quad \text{with} \quad \mathbf{V}^i_j = V^{\delta_{1,i}}_j \otimes \cdots \otimes V^{\delta_{d,i}}_j, \;\; 1 \leq i \leq d, \tag{62}$$

where $\delta_{i,j}$ denotes the Kronecker symbol. To satisfy the free-slip boundary condition we must replace V^1_j by $V^{1,0}_j$ in (62). We also emphasized that, the corresponding spaces $\vec{\mathbf{V}}^{div}_j = \vec{\mathbf{V}}_j \cap \mathcal{H}_{div}(\Omega) = \vec{\mathbf{P}}_j(\mathcal{H}_{div}(\Omega))$ provide a multiresolution analysis of $\mathcal{H}_{div}(\Omega)$. Following a similar approach as for $d = 3$, and taking the $(d-1)$ scaling functions that generated the previous divergence-free wavelets, we obtain a divergence-free scaling functions basis of $\vec{\mathbf{V}}^{div}_j$.

7. Conclusion

In this paper we have presented a new construction of biorthogonal wavelet bases linked by differentiation and integration. In opposite to the existing constructions, the differentiation relation between the wavelet basis $\psi^1_{j,k}$ and $\psi^0_{j,k}$ remains diagonal as for the internal wavelet, and including an homogeneous boundary condition on the boundary. Several experiments have demonstrated

the potential applications of this new construction in signal compression and in the numerical resolution of the Poisson equation in one dimensional space. Moreover, the diagonal relation between the wavelet bases improves the complexity of the fast divergence-free wavelet transform algorithms.

References

[1] L. Andersson, N. Hall, B. Jawerth, G. Peters, Wavelets on closed subsets of the real line, *Recents Advances in Wavelets Analysis (L.L. Schumaker and G. Webb eds)*, Academic Press (1993) 1–61.

[2] G. Beylkin, On the representation of operator in bases of compactly supported wavelets, *SIAM J.Numer.Anal.* **6(6)** (1992) 1716–1740.

[3] C. Canuto, R. Masson, Stabilized wavelet approximations of the Stokes problem, *Math. of Comput.* **70(236)** (2000) 1397–1416.

[4] A. Cohen, I. Daubechies, J.-C. Feauveau,Biorthogonal bases of compactly supported wavelets, *Comm. Pure Appli. Maths.* **45** (1992) 485–560.

[5] A. Cohen, I. Daubechies, P. Vial, Wavelets on the Interval and Fast Wavelet Transforms, *Appl. Comput. Harmon. Anal.* **1** (1993) 54–81.

[6] W. Dahmen, A. Kunoth, K. Urban, A wavelet Galerkin method for the Stokes equations , *Computing.* **3 (56)** (1996) 259–301.

[7] W. Dahmen, A. Kunoth, K. Urban, Biorthogonal Spline-wavelets on the interval. Stability and moment conditions, *App. Comput. Harmon. Anal.* **6** (1999) 132–196.

[8] I. Daubechies, Orthogonal bases of compactly supported wavelets, *Comm. Pure and Appli. Math.* **7 (41)** (1988) 906–996.

[9] E. Deriaz, V. Perrier, Orthogonal Helmholtz decomposition in arbitrary dimension using divergence-free and curl-free wavelets, *App. Comput. Harmon. Anal.*, **26** (2009) 249–269.

[10] M. Fortin, An analysis of the convergence of mixed finite element methods, *ESAIM: Mathematical Modelling and Numerical Analysis* **4 (11)** (1977) 341–354.

[11] S. Grivet-Talocia, A. Tabacco, Wavelet on the interval with optimal localization, *Math. Models. Meth. Appl. Sci.* **10(3)** (2000) 441–462.

[12] W. Hager, Applied Numerical Linear Algebra, *Prentice-Hall,* (1988).

[13] A. Jouini, P.G. Lemarié-Rieusset, Analyse multirésolution biorthogonale sur l'intervalle et applications, *Annales de l'I.H.P. Section C* **10** (1993) 453–476.

[14] P.G. Lemarié-Rieusset, Analyses multi-résolutions non orthogonales, commutation entre projecteurs et dérivation et ondelettes vecteurs à divergence nulle, *Revista Matemática Iberoamericana* **8(2)** (1992) 221–236.

[15] R. Masson, Biorthogonal spline wavelets on the interval for the resolution of boundary problems, *M3AS.* **6** (6) (1996) 749–791.

[16] P. Monasse, V. Perrier, Orthogonal Wavelet Bases Adapted For Partial Differential Equations With Boundary Conditions, *SIAM J.Math. Anal.* **29** (1998) 1040–1065.

[17] S. Kadri-Harouna, $http://pageperso.univ-lr.fr/souleymane.kadri\_harouna/Softwares.html$

[18] S. Kadri-Harouna, V. Perrier, Divergence-free Wavelet Projection Method for Incompressible Viscous Flow, *SIAM Multiscale Modeling and Simulation* **13(1)** (2015) 399–422.

[19] S. Kadri-Harouna, V. Perrier, Effective construction of divergence-free wavelets on the square, *J. of Computational and Applied Math.* **240** (2013) 74–86.

[20] S. Kadri-Harouna, V. Perrier, Helmholtz-Hodge Decomposition on $[0,1]^d$ by Divergence-free and Curl-free Wavelets, *Lecture Notes in Computer Science series* **6920** (2012), springer, 311–329.

[21] R. Stevenson, Divergence-free wavelet bases on the hypercube: Free-slip boundary conditions, and applications for solving the instationary Stokes equations, *Math. Comp.* **80** (2011) 1499–1523.

[22] R. Stevenson, Divergence-free wavelet bases on the hypercube, *Appl. Comput. Harmon. Anal.* **30** (2011) 1–19.

[23] K. Urban, Wavelet Bases in H(div) and H($curl$), *Math. Comput.* **70** (2000) 739–766.